CHIRALITY 2026

The 10th International Conference on Chirality, Vorticity, and Magnetic Field in Quantum Matter

FUDAN UNIVERSITY

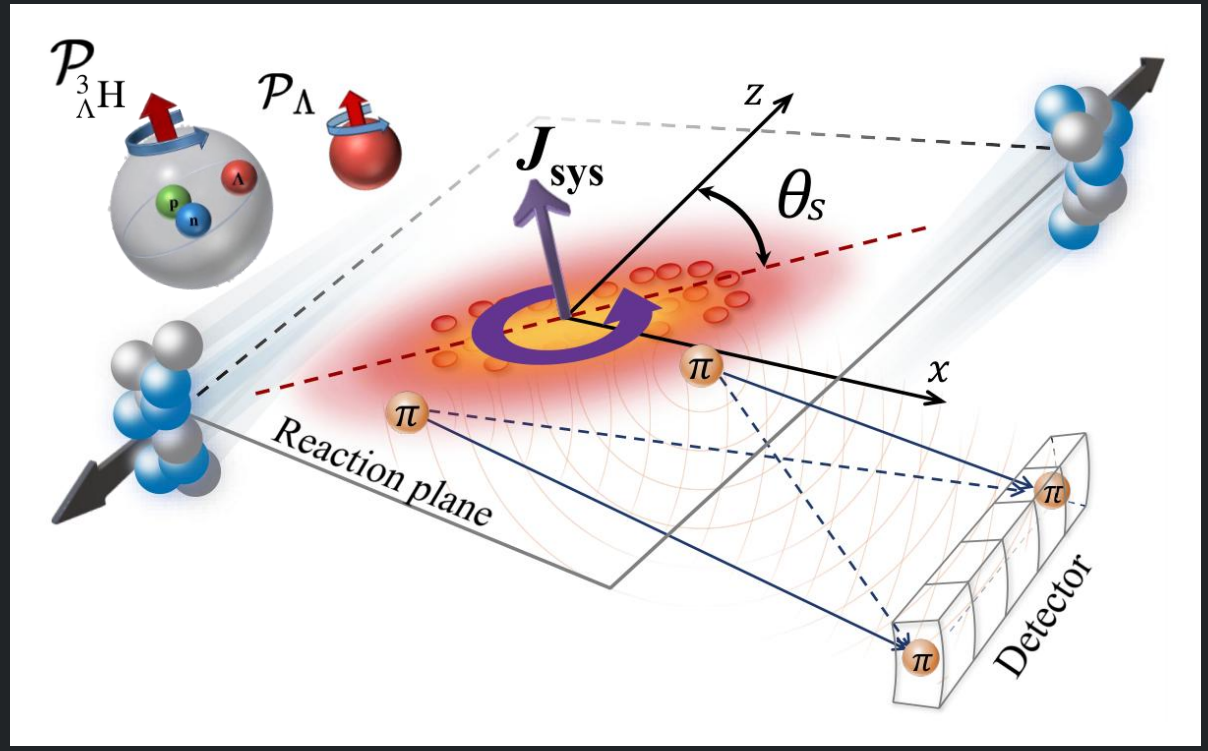
Spin Polarizations of Light (Hyper-)Nuclei in Tilted Nuclear Matter

Kai-Jia Sun

Fudan University

November 17, 2026

In collaboration with Jan Steinheimer, Marcus Bleicher, Dai-Neng Liu, Yun-Peng Zheng, Jun Xu, Song Zhang, Jin-Hui Chen, Lie-Wen Chen, Yu-Gang Ma, and Che-Ming Ko



The 7th International Conference on Chirality, Vorticity and Magnetic Field in Heavy Ion Collisions

University of Chinese Academy of Sciences **Jul 15 – 19, 2023**



Inspired by this workshop, I began exploring emergent spin phenomena(缘起)

Outline

I Background: spin polarization and rotation

II A geometry-modulated Barnett-like effect

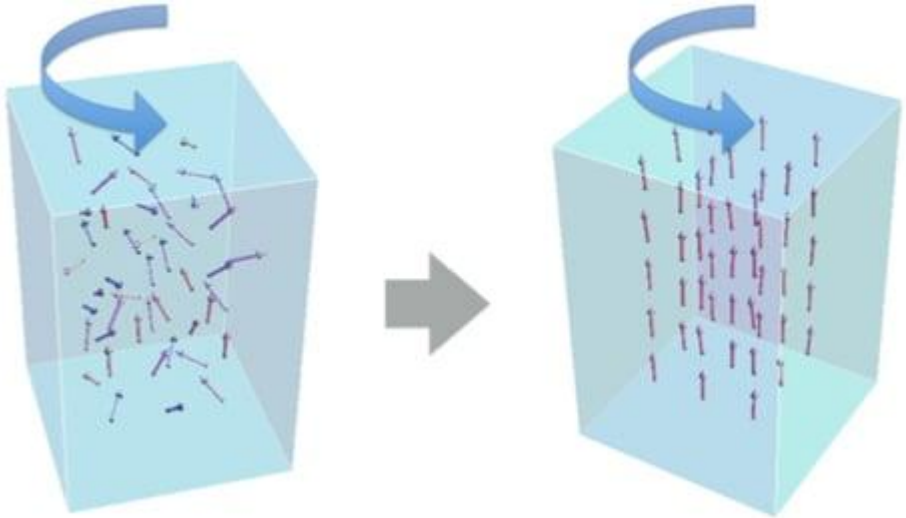
III Spin polarization of (anti-)(hyper-)nuclei

IV Summary and outlook

Spin polarization and rotation

Barnett effect

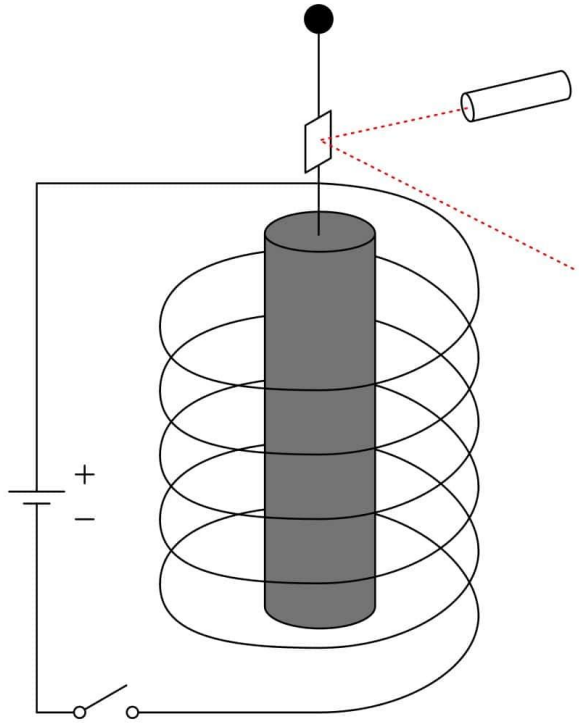
Rotation → magnetization



Barnett, Phys Rev. (1915) 6:239–70.

Einstein-de Haas effect

Magnetization → rotation



A. Einstein and W. J. de Haas, Verh. Deut. Phys. Ges. 17, 152 (1915).

Spin polarization from quarks to hadrons in heavy-ion collisions

Z. T. Liang and X. N. Wang PRL 94, 102301 (2005)

Globally Polarized Quark-Gluon Plasma in Noncentral $A + A$ Collisions

Zuo-Tang Liang[1] and Xin-Nian Wang[2,1]

Produced partons have a large local relative orbital angular momentum along the direction opposite to the reaction plane in the early stage of noncentral heavy-ion collisions. Parton scattering is shown to polarize quarks along the same direction due to spin-orbital coupling. Such global quark polarization will lead to many observable consequences, such as left-right asymmetry of hadron spectra and global transverse polarization of thermal photons, dileptons, and hadrons. Hadrons from the decay of polarized resonances will have an azimuthal asymmetry similar to the elliptic flow. Global hyperon polarization is studied within different hadronization scenarios and can be easily tested.

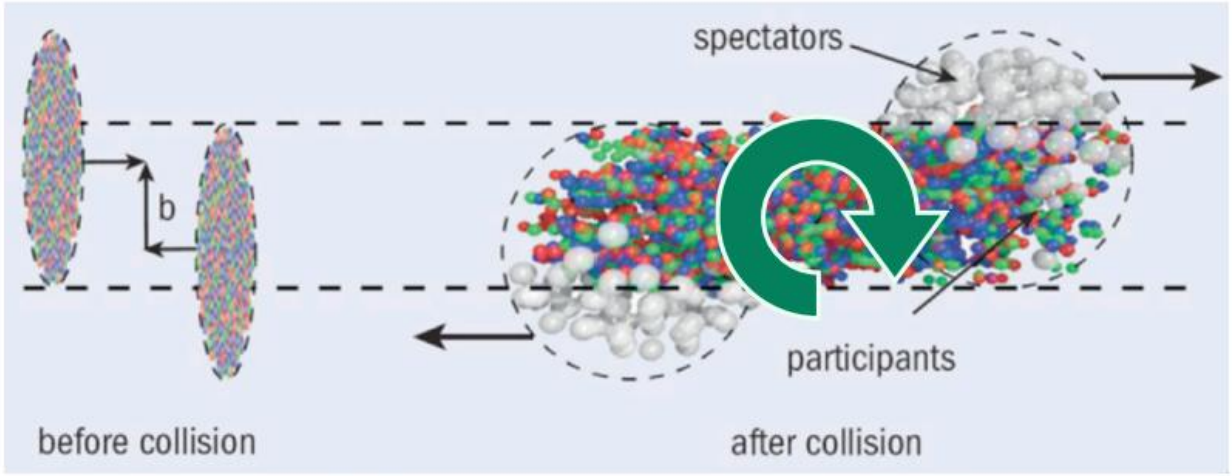


figure: M. Lisa, talk @ "Strangeness in Quark Matter 2016"

F. Becattini, F. Piccinini, Annals of Physics 323, 2452 (2008)

The ideal relativistic spinning gas: Polarization and spectra

F. Becattini [a,*], F. Piccinini [b]

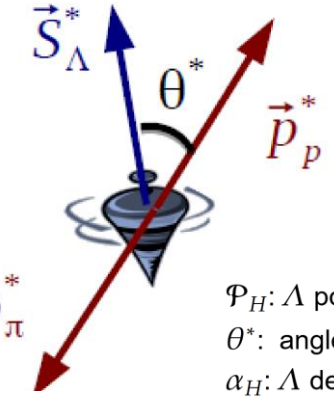
$$\hat{\rho}_\omega = \frac{1}{Z_\omega} \exp[(-\hat{h} + \mu\hat{q} + \boldsymbol{\omega}\cdot\hat{\mathbf{j}})/T]\mathrm{P}_V$$

$$\mathbf{\Pi} = \mathrm{tr}[\hat{\mathbf{S}}\hat{\rho}_\omega(p)] = \frac{\sum_{n=-S}^{S} n\mathrm{e}^{n\omega/T}}{\sum_{n=-S}^{S} \mathrm{e}^{n\omega/T}}\hat{\boldsymbol{\omega}}$$

Vorticity ⟸ **Spin polarization**

$$\omega \approx k_\mathrm{B}T(\overline{\mathcal{P}}_\Lambda + \overline{\mathcal{P}}_{\overline{\Lambda}})/\hbar$$

Global spin polarization of Lambda hyperon in heavy-ion collisions



$$\Lambda \to p + \pi^-$$

$$\frac{dN}{d\cos\theta^*} = \mathrm{Tr}[T^+ \hat{\rho} T]$$

$$\rho_\Lambda = \begin{pmatrix} \frac{1+\mathcal{P}_\Lambda}{2} & \\ & \frac{1-\mathcal{P}_\Lambda}{2} \end{pmatrix}$$

$\mathcal{P}_H$: Λ polarization

θ^*: angle between proton momentum in Λ rest frame

α_H: Λ decay parameter

$\alpha_\Lambda = 2\mathrm{Re}(T_s^* T_p) = 0.732 \pm 0.014$

BESIII, Phys. Rev. Lett. 129, 131801 (2022).

The transition matrix

$$T(\Lambda \to \pi^- + p) = \frac{1}{\sqrt{4\pi}} \begin{pmatrix} T_s + T_p \cos\theta_p^* & T_p \sin\theta_p^* e^{i\phi_p^*} \\ T_p \sin\theta_p^* e^{-i\phi_p^*} & T_s - T_p \cos\theta_p^* \end{pmatrix}$$

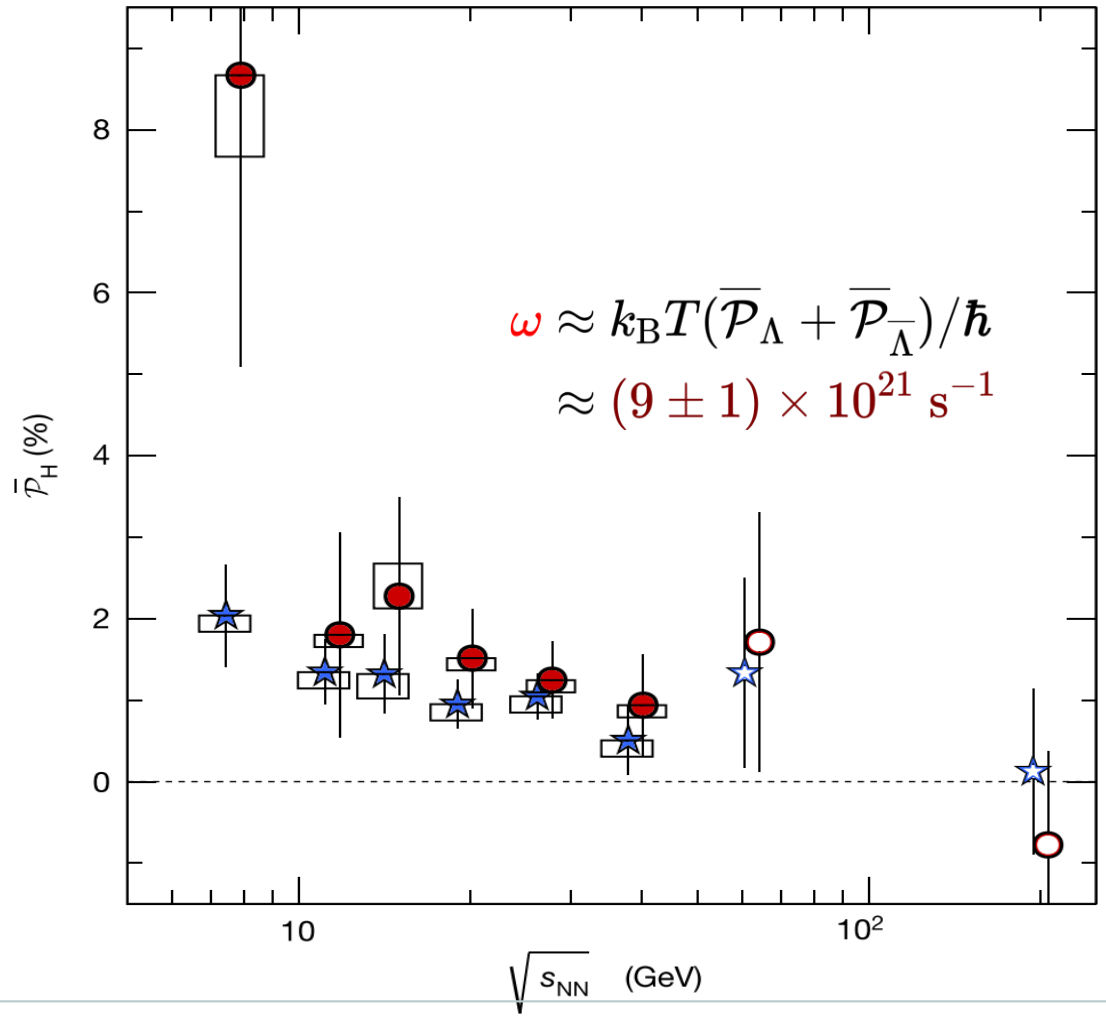
The angular distribution

$$\frac{dN}{d\cos\theta^*} = \frac{1}{2}(1 + \alpha_\Lambda |\mathcal{P}_\Lambda| \cos\theta^*)$$

Decay constant — Spin polarization

Parity-violating weak decay

STAR, Nature 548, 62 (2017)

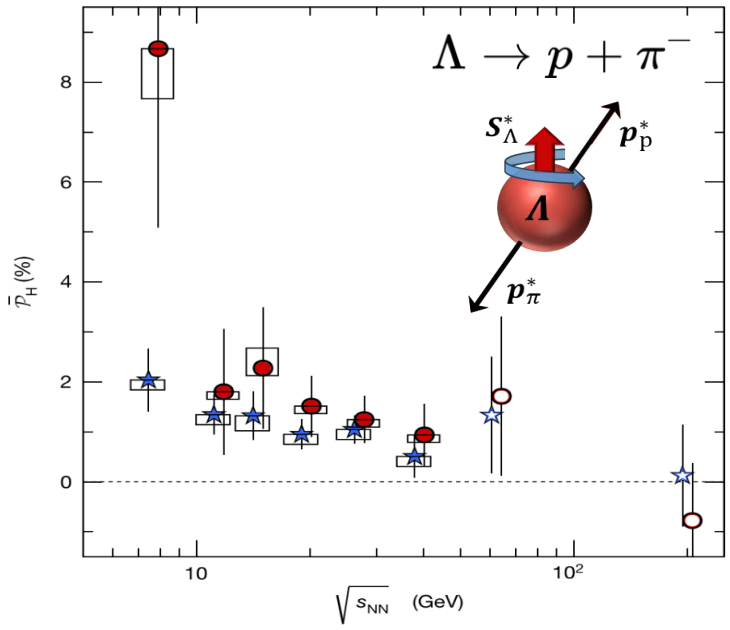


Spin polarization of Lambda hyperon ➡ **Vorticity of QGP**

Spin measurements now probe more than polarization

2017

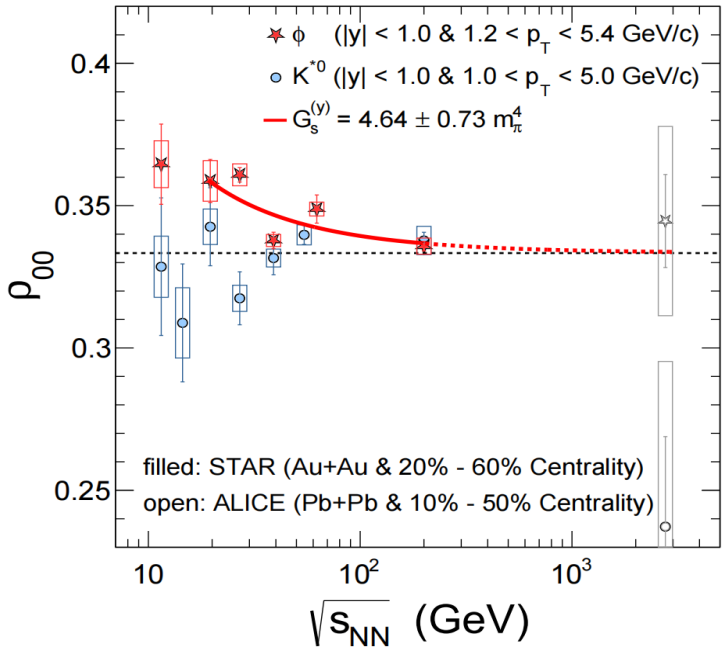
Global polarization



Mean spin orientation

2023

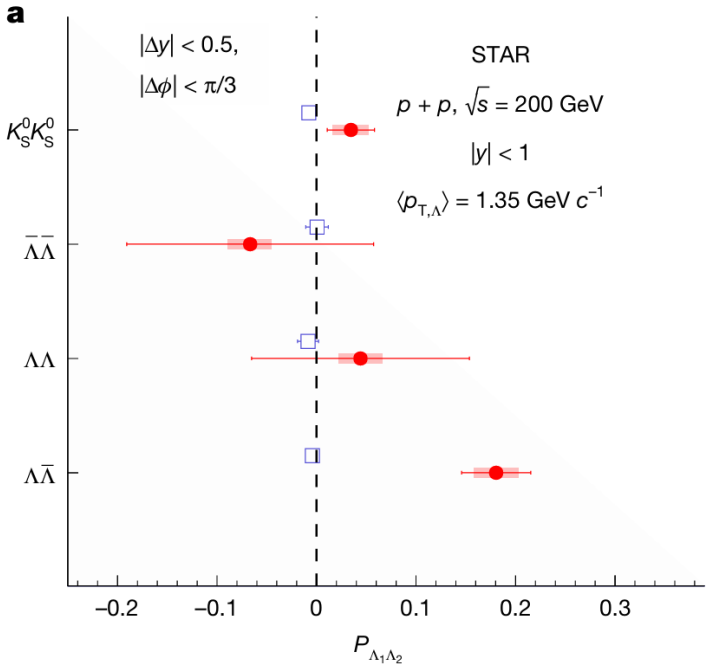
Vector-meson alignment



Spin-state populations

2026

Hyperon-pair correlations



Correlations between spins

Polarization, alignment, and correlations are complementary spin observables.

STAR, Nature 548, 62 (2017); Nature 614, 244 (2023); Nature 650, 5 (2026).

Outline

I Background: spin polarization and rotation

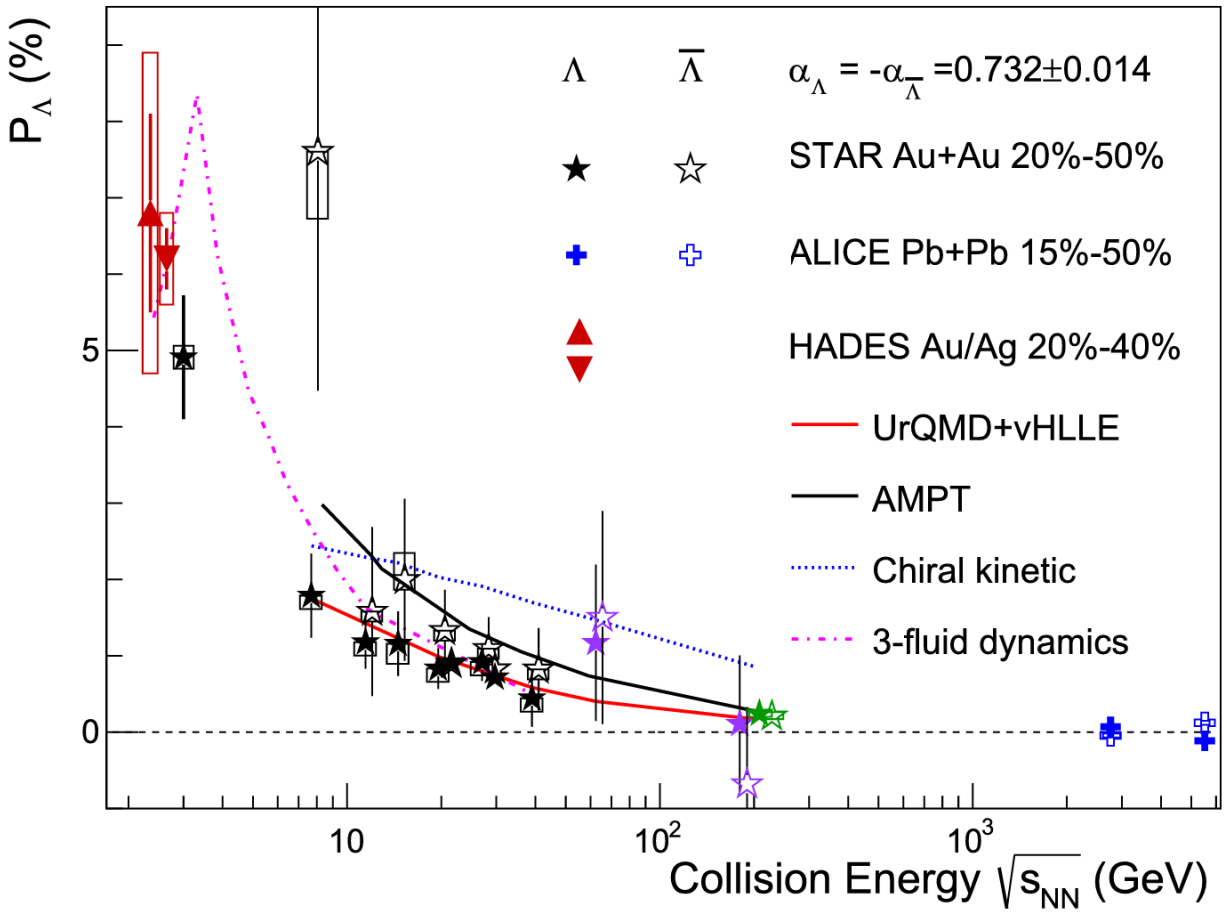
II A geometry-modulated Barnett-like effect

III Spin polarization of (anti-)(hyper-)nuclei

IV Summary and outlook

Correlation between global polarization and source tilt

J. Chen et al., Nucl. Sci. Tech. 35, 214 (2024)
F. Becattini et al., Int. J. Mod. Phys. E 33(06), 2430006 (2024)
C. Yi et al., arXiv:2603.27521

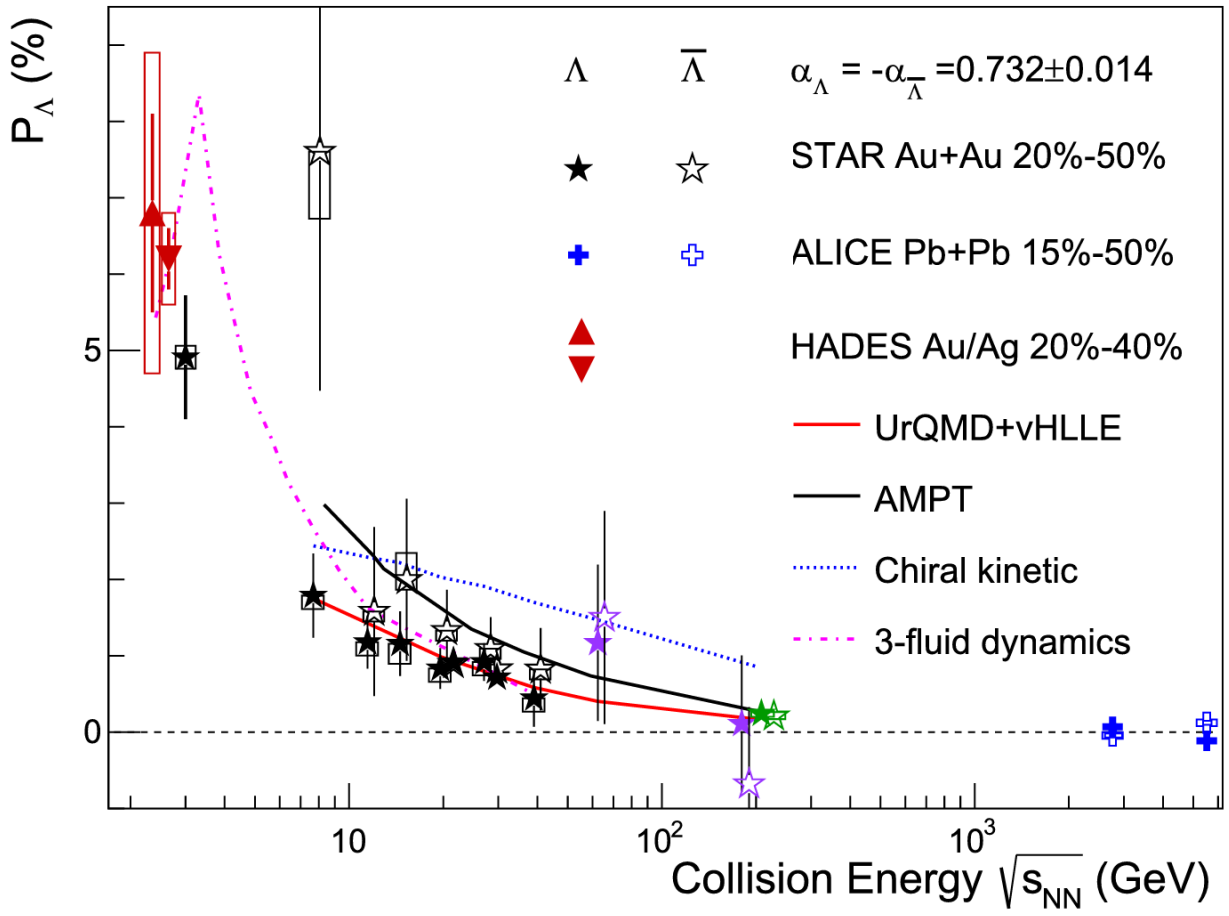


The decrease trend of global Lambda polarization was understood as deposit of smaller fraction of angular momentum in the mid-rapidity at higher collision energy (See talk by Jin-Feng Liao)

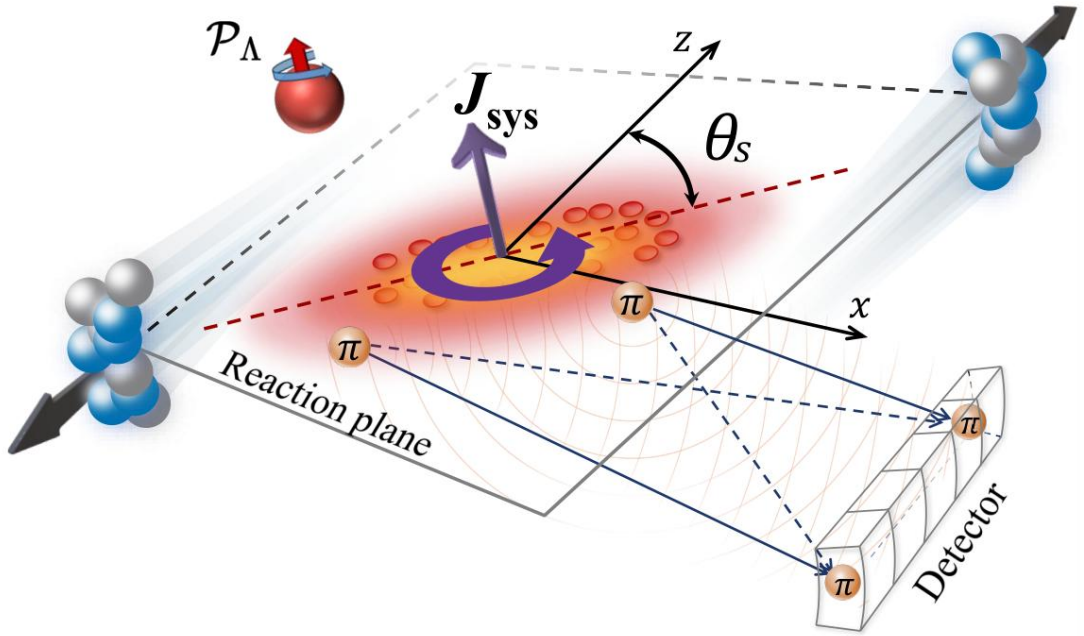
But some studies show that global polarization is not directly correlated with mid-rapidity angular momentum [Y. B. Ivanov and A. A. Soldatov, Phys. Rev. C 102 (2020) 2, 024916]

Correlation between global polarization and source tilt

J. Chen et al., Nucl. Sci. Tech. 35, 214 (2024)
F. Becattini et al., Int. J. Mod. Phys. E 33(06), 2430006 (2024)
C. Yi et al., arXiv:2603.27521



D. N. Liu, K. J. Sun, J. Steinheimer, J. H. Chen, Y. G. Ma, and M. Bleicher, arXiv:2610.35310 (2026)



Geometric modulation on spin polarization

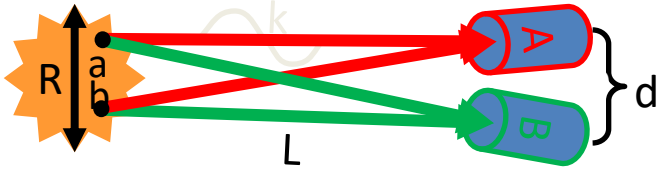
$$P_\Lambda \propto |\varpi_{zx}|\,\theta_s$$

Source geometry helps explain the energy dependence of polarization

Source geometry from correlation femtoscopy

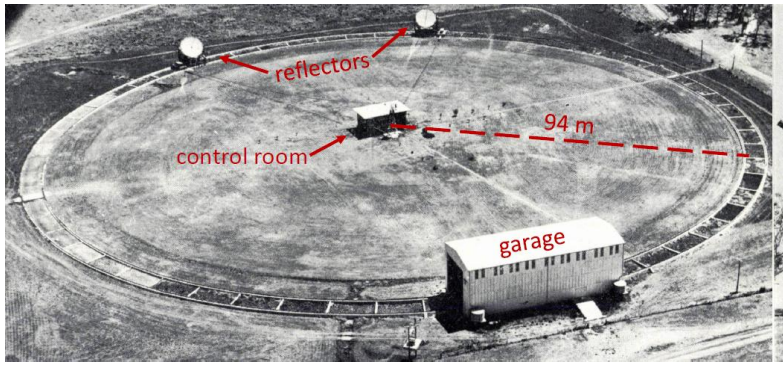
Hanbury Brown-Twiss (HBT) intensity interferometry

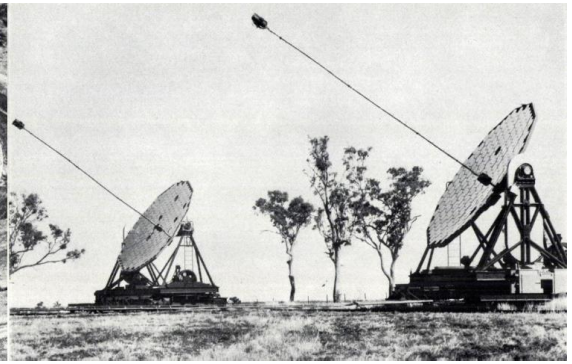
Nature 178, 1046 (1956)

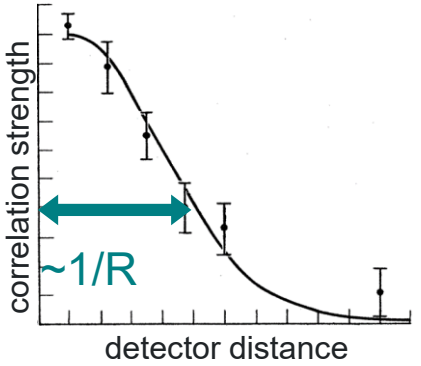


$$C_{AB}(\Delta) = \frac{\langle I_A I_B \rangle}{\langle I_A \rangle \langle I_B \rangle} = 1 + \frac{1}{2}\cos\frac{kRd}{L}$$

$R_{\mathrm{Star}} \sim 10^{8} - 10^{11} m$

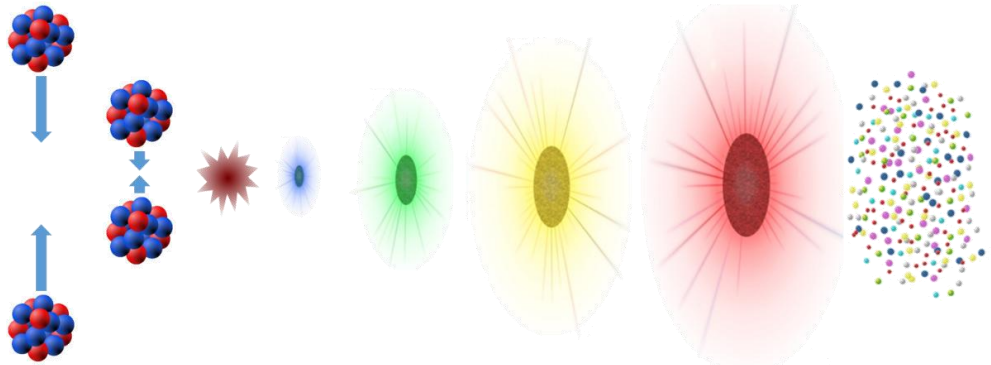


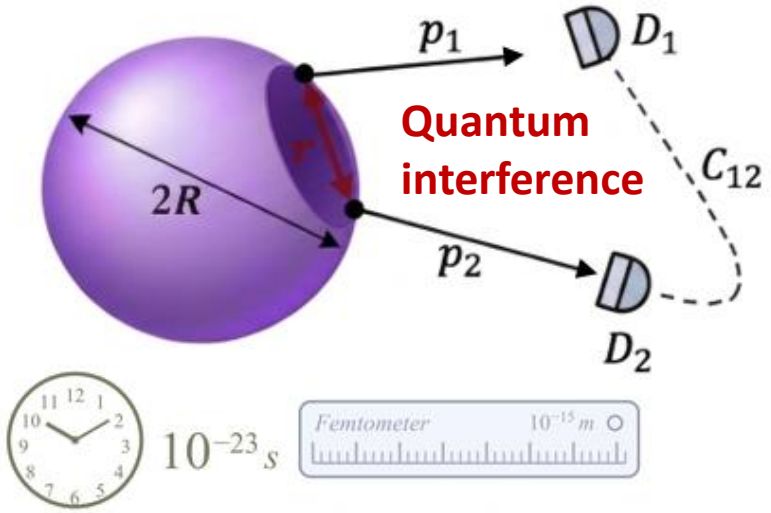


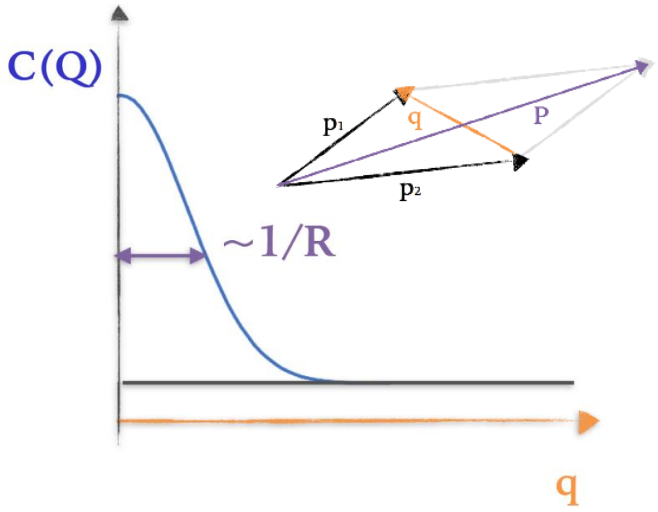


Correlation Femtoscopy

$R_{\mathrm{HIC}} \sim 10^{-15}\ m$







U. Heinz and B. Jacak, Ann. Rev. Nucl. Part. Sci. 49, 529 (1999)

Source tilt angle from azimuthally sensitive femtoscopy (asHBT)

1 Two-pion correlations

$$C(\boldsymbol{k},\boldsymbol{K}) = \frac{\int d\Sigma\ S_1(x_1,\boldsymbol{p}_1)S_2(x_2,\boldsymbol{p}_2)|\psi_{\boldsymbol{k}}(\boldsymbol{x})|^2}{\int d\Sigma\ S_1(x_1,\boldsymbol{p}_1)S_2(x_2,\boldsymbol{p}_2)}$$

$$C(\boldsymbol{k},\boldsymbol{K},\phi) = 1+\lambda(\boldsymbol{K})\exp\left[-\sum_{i,j=o,s,l} k_i k_j R_{ij}^2(\boldsymbol{K},\phi)\right]$$

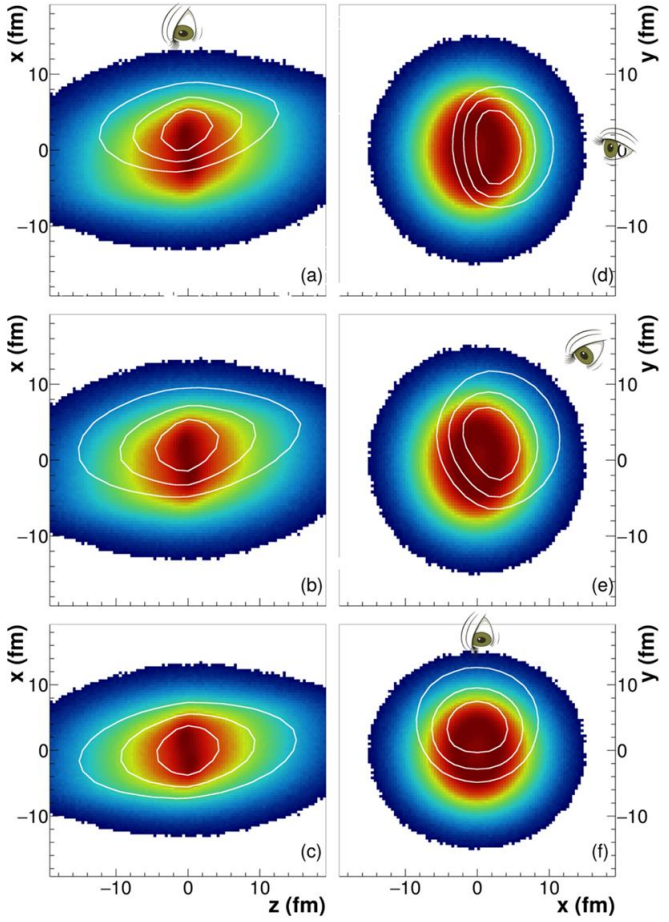
2 Fit azimuthally dependent HBT radii

The radius oscillations encode the spatial orientation of the emitting region.

3 Extract the tilt angle

$$\theta_s \simeq \frac{1}{2}\tan^{-1}\left[\frac{-4R_{sl,1}^2}{R_{l,0}^2 - R_{s,0}^2 + 2R_{s,2}^2}\right]$$

Reconstructed source geometry



Momentum correlations provide access to the orientation of the emission source.

M. A. Lisa et al., Phys. Lett. B 489, 287 (2000); STAR, arXiv:2605.15013; D.-N. Liu et al., arXiv:2610.35310.

Source tilt angle from azimuthally sensitive femtoscopy (asHBT)

$$S \propto \exp\left(-\frac{(x\cos\theta_s - z\sin\theta_s)^2}{2\sigma_{x'}^2} - \frac{y^2}{2\sigma_y^2} - \frac{(x\sin\theta_s + z\cos\theta_s)^2}{2\sigma_{z'}^2} - \frac{t^2}{2\sigma_t^2}\right)$$

$$R_o^2(\phi) = R_{o,0}^2 + 2\sum_{n=2,4,6,\ldots} R_{o,n}^2\cos(n\phi),$$

$$R_s^2(\phi) = R_{s,0}^2 + 2\sum_{n=2,4,6,\ldots} R_{s,n}^2\cos(n\phi),$$

$$R_l^2(\phi) = R_{l,0}^2 + 2\sum_{n=2,4,6,\ldots} R_{l,n}^2\cos(n\phi),$$

$$R_{os}^2(\phi) = 2\sum_{n=2,4,6,\ldots} R_{os,n}^2\sin(n\phi),$$

$$R_{ol}^2(\phi) = 2\sum_{n=1,3,5,\ldots} R_{ol,n}^2\cos(n\phi),$$

$$R_{sl}^2(\phi) = 2\sum_{n=1,3,5,\ldots} R_{sl,n}^2\sin(n\phi).$$

$$\langle\tilde{x}_i^2\rangle = R_{s,0}^2 - 2R_{s,2}^2,$$

$$\langle\tilde{z}_i^2\rangle = R_{l,0}^2,$$

$$\langle\tilde{x}_i\tilde{z}_i\rangle = -2R_{sl,1}^2.$$

$$\theta_s = \frac{1}{2}\tan^{-1}\left(\frac{2\langle\tilde{x}\tilde{z}\rangle}{\langle\tilde{z}^2\rangle - \langle\tilde{x}^2\rangle}\right),$$

$$\approx \frac{1}{2}\tan^{-1}\left(\frac{-4R_{sl,1}^2}{R_{l,0}^2 - R_{s,0}^2 + 2R_{s,2}^2}\right)$$

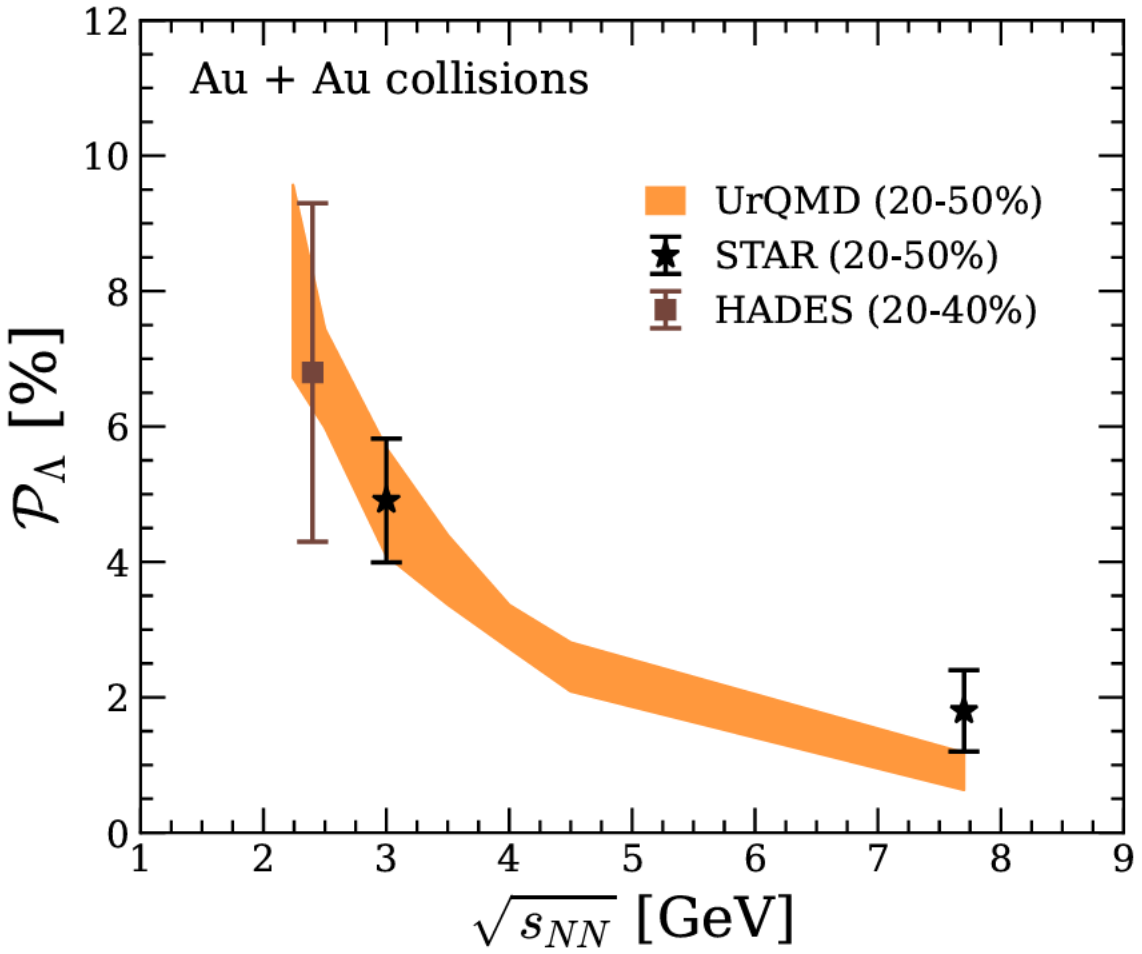
Momentum correlations provide access to the orientation of the emission source.

M. A. Lisa et al., Phys. Lett. B 489, 287 (2000); STAR, arXiv:2605.15013; D.-N. Liu et al., arXiv:2610.35310.

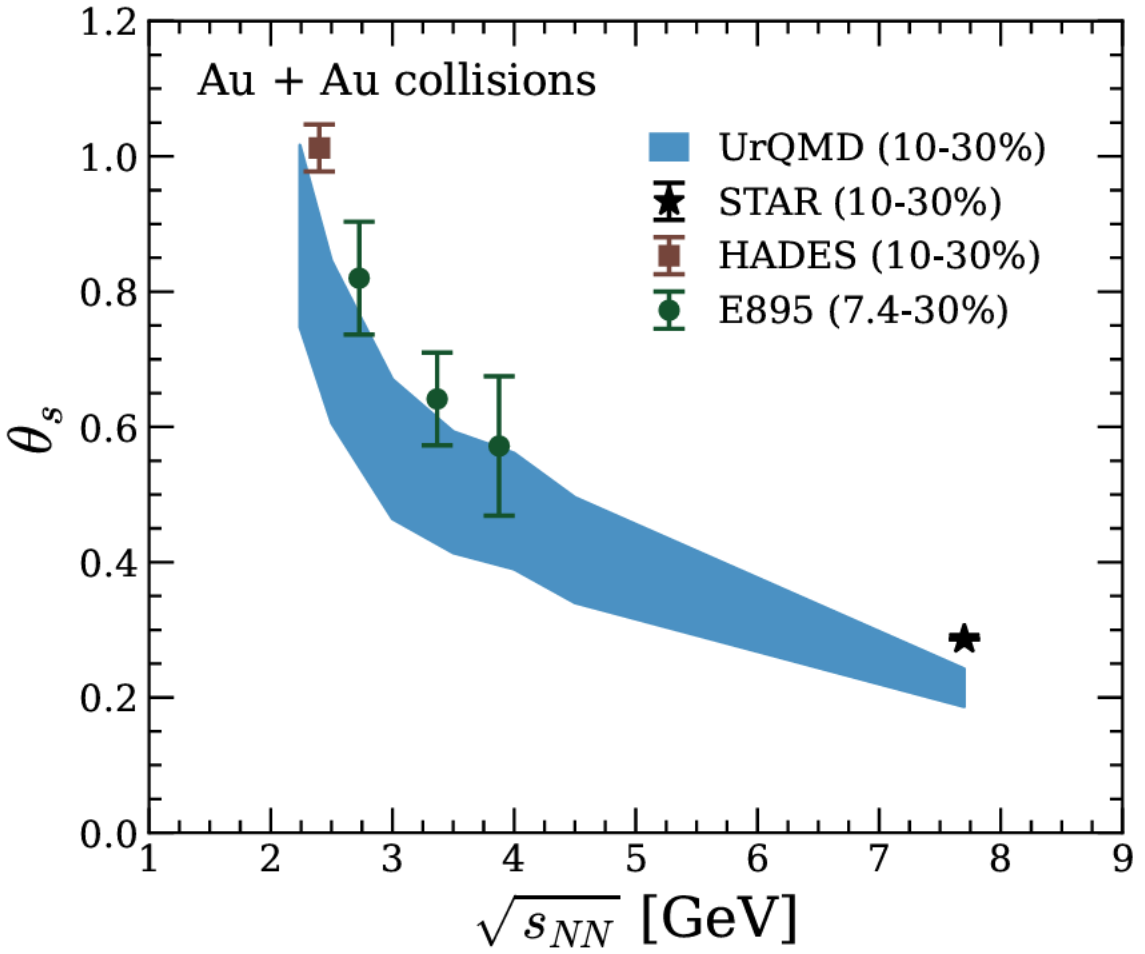
Energy dependence

D. N. Liu, K. J. Sun, J. Steinheimer, J. H. Chen, Y. G. Ma, and M. Bleicher, arXiv:2610.35310 (2026)

a Global polarization



b Source tilt angle

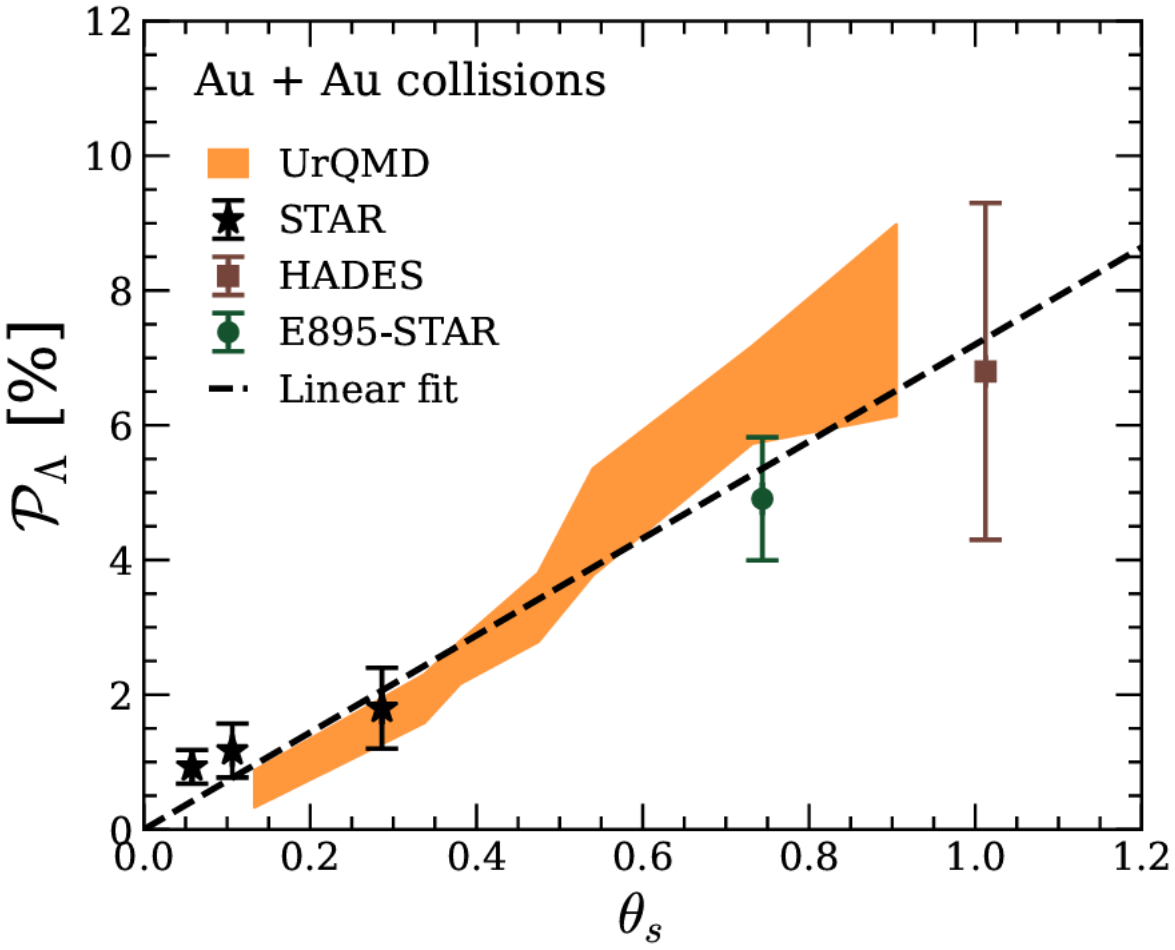


$$\mathcal{P}^\mu(x,p) = -\frac{1}{4m}(1-n_F)\epsilon^{\mu\nu\rho\sigma}p_\nu\varpi_{\rho\sigma}(x) \qquad \mathcal{P}_\Lambda = \langle\frac{\boldsymbol{\mathcal{P}}^*\cdot\boldsymbol{J}_{\rm sys}}{|\boldsymbol{J}_{\rm sys}|}\rangle$$

$$\mathcal{P}^\mu = (0,\boldsymbol{\mathcal{P}}^*)$$

A geometry-modulated Barnett-like effect

D. N. Liu, K. J. Sun, J. Steinheimer, J. H. Chen, Y. G. Ma, and M. Bleicher, arXiv:2610.35310 (2026)



Linear fit to the experimental points

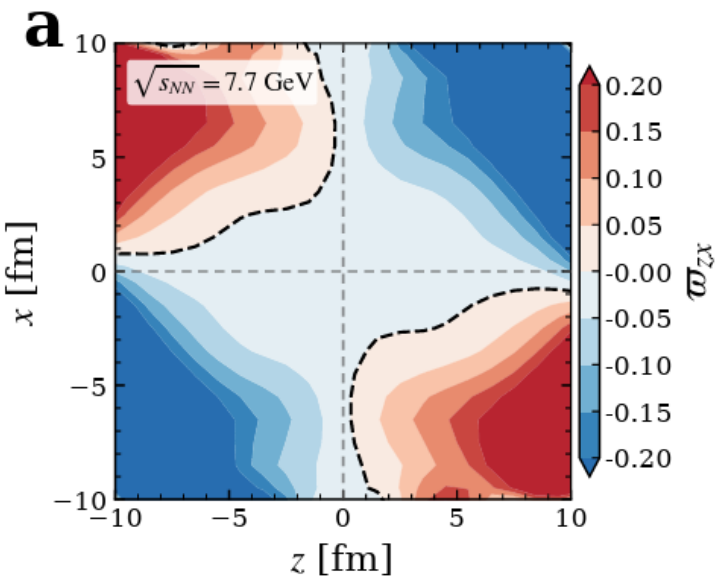
$$P_\Lambda = (0.072 \pm 0.010)\,\theta_s$$

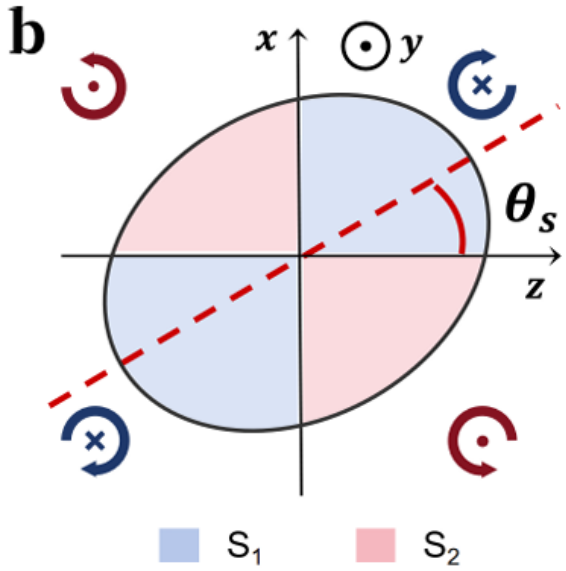
Global Lambda polarization is modulated by the source geometry

A geometry-modulated Barnett-like effect

D. N. Liu, K. J. Sun, J. Steinheimer, J. H. Chen, Y. G. Ma, and M. Bleicher, arXiv:2610.35310 (2026)

Opposite local contributions





Geometric modulation

Vorticity changes sign across the source; without tilt, the contributions almost cancel.

A finite tilt leaves a residual

$$\mathcal{P}_\Lambda = \frac{E}{2m}\frac{2(R_a^2 - R_b^2)}{\pi R_a R_b}|\varpi_{zx}|\theta_s$$

The residual is proportional to θs at leading order, and vanishes with increasing energy.

Similar pattern seen in H. Li et al., Phys. Rev. C 96(5), 054908 (2017)

The spin response depends jointly on local thermal vorticity and source geometry.

Outline

I Background: spin polarization and rotation

II A geometry-modulated Barnett-like effect

III Spin polarization of (anti-)(hyper-)nuclei

IV Summary and outlook

From polarization of hadrons to light (hyper-)nuclei

K. J. Sun et al., Phys. Rev. Lett. 134, 022301 (2025)

K. J. Sun, R. Wang, C. M. Ko, Y. G. Ma, C. Shen, Nature Commun. 15, 1074 (2024)

R.-J. Liu and J. Xu, Phys. Rev. C 109, 014615 (2024).

Elementary hadrons

$\Lambda(uds)$ $\Xi(uss)$ $\Omega(sss)$

$\phi(s\bar{s})$ $K^{*0}(d\bar{s})$ $\rho^{+}(u\bar{d})$

$J/\psi(c\bar{c})$ ...

Stable (anti-)nuclei

Spin $\frac{1}{2}$ 1 $\frac{1}{2}$

$p(uud)$ $d(np)$ $^{3}\mathrm{He}(npp)$

$\bar{p}(\bar{u}\bar{u}\bar{d})$ $\bar{d}(\bar{n}\bar{p})$ $^{3}\overline{\mathrm{He}}(\bar{n}\bar{p}\bar{p})$

Unstable (anti-)(hyper-)nuclei

Spin $\frac{1}{2}, \frac{3}{2}$? $2\ (g.s.)$

$^{3}_{\Lambda}\mathrm{H}(np\Lambda)$ $^{4}\mathrm{Li}(\mathrm{nppp})$

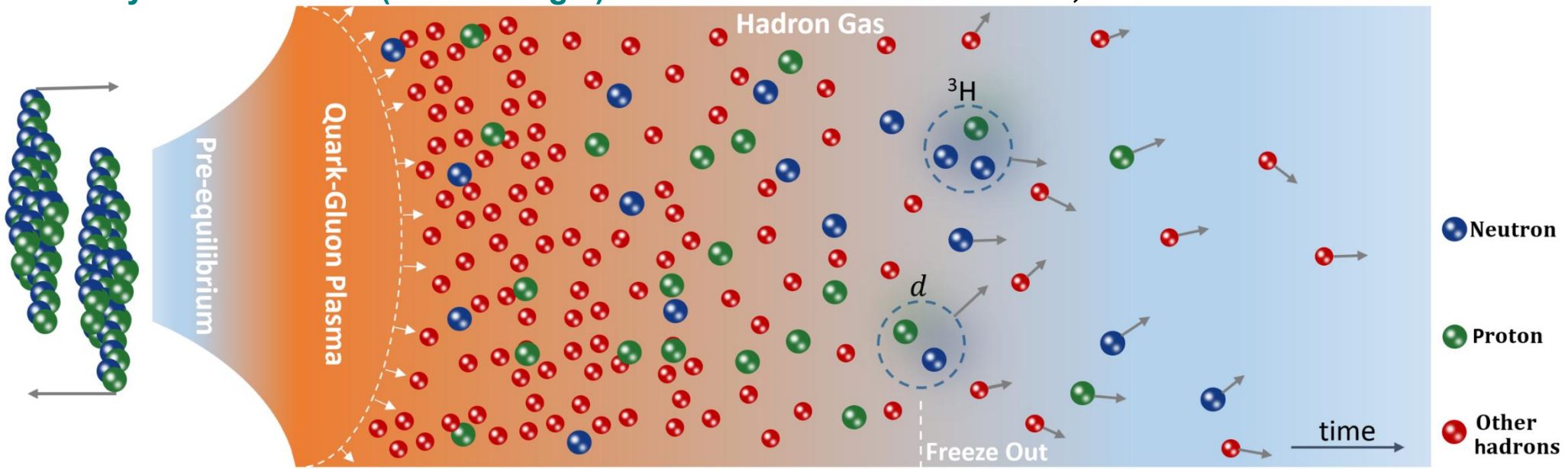
$^{3}_{\Lambda}\overline{\mathrm{H}}(\bar{n}\bar{p}\bar{\Lambda})$ $^{4}\overline{\mathrm{Li}}(\bar{n}\bar{p}\bar{p}\bar{p})$

...

From polarization of hadrons to light (hyper-)nuclei

Relativistic Heavy-Ion Collisions ('Little Bangs')

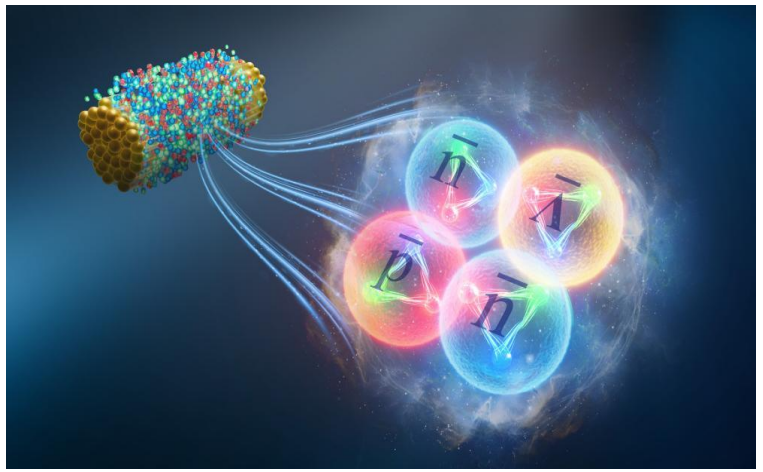
$t \sim 10^{-23} s, T \sim 100$ MeV

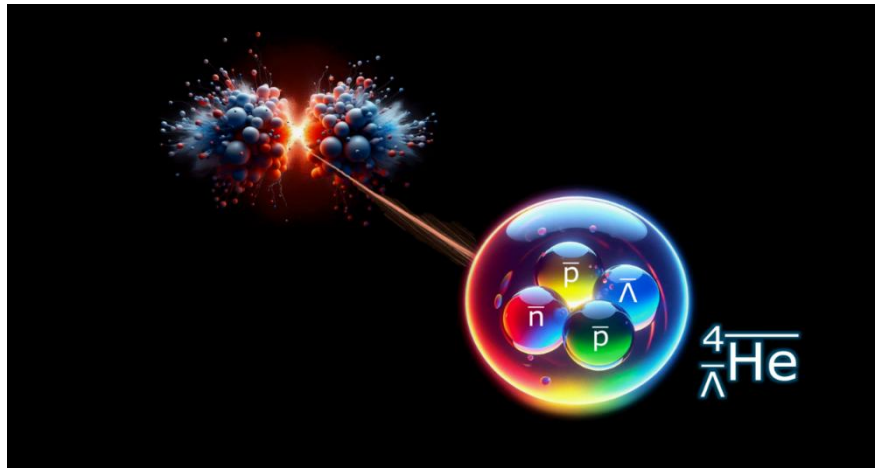


K. J. Sun, R. Wang, C. M. Ko, Y. G. Ma, C. Shen, Nature Commun. 15, 1074 (2024)



ALICE, PRL 134, 162301 (2025)

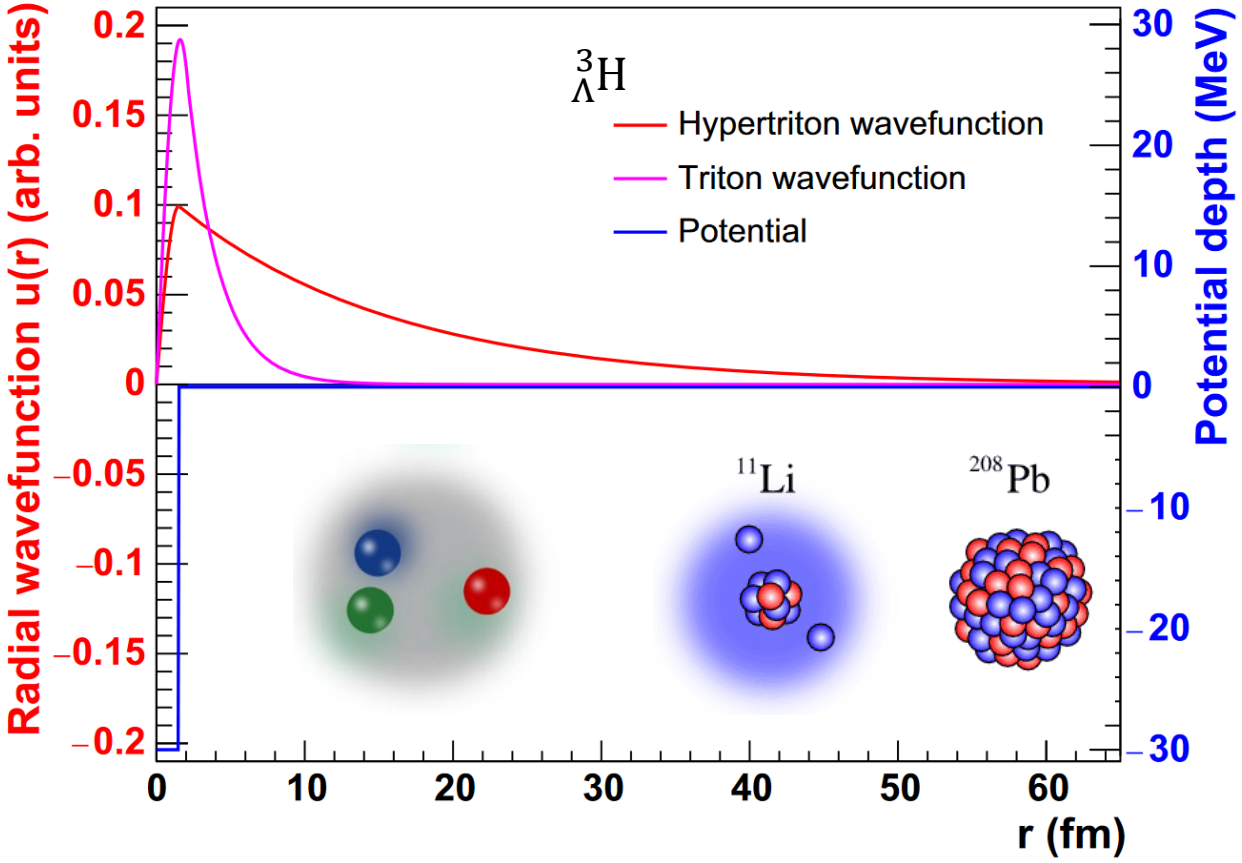




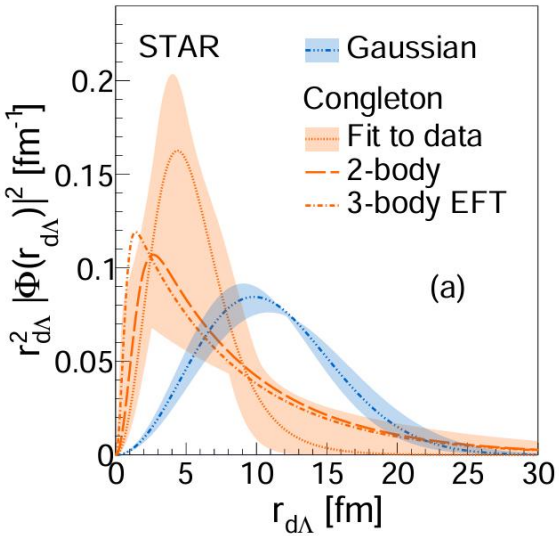
Little bangs produce nearly equal amounts of matter and antimatter light nuclei.

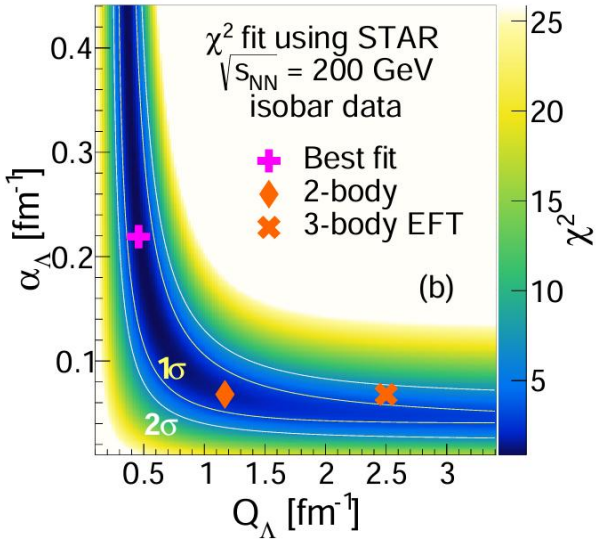
Strange halo nucleus: (anti-)hypertriton

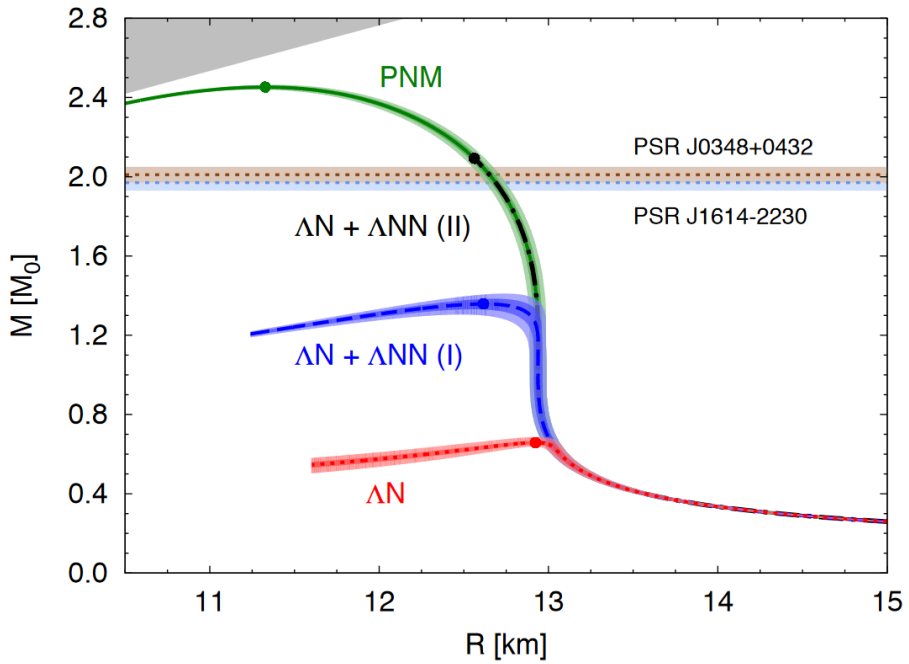
A halo-like spatial structure



STAR, arxiv:2607.28113







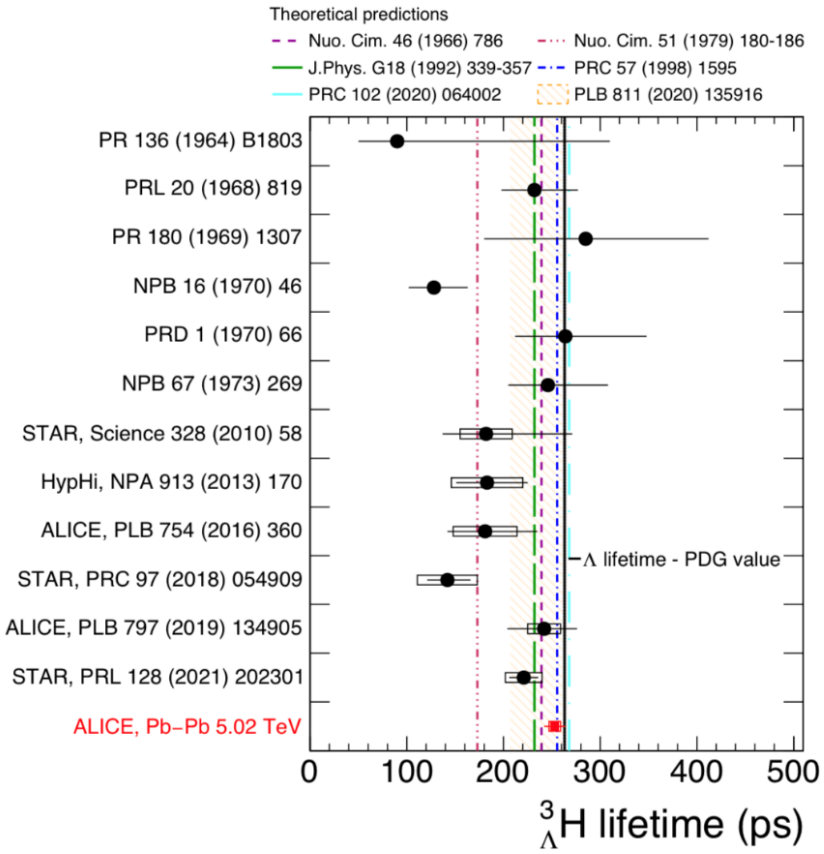
D. Lonardoni et al., Phys.Rev.Lett. 114 (2015) 9, 092301

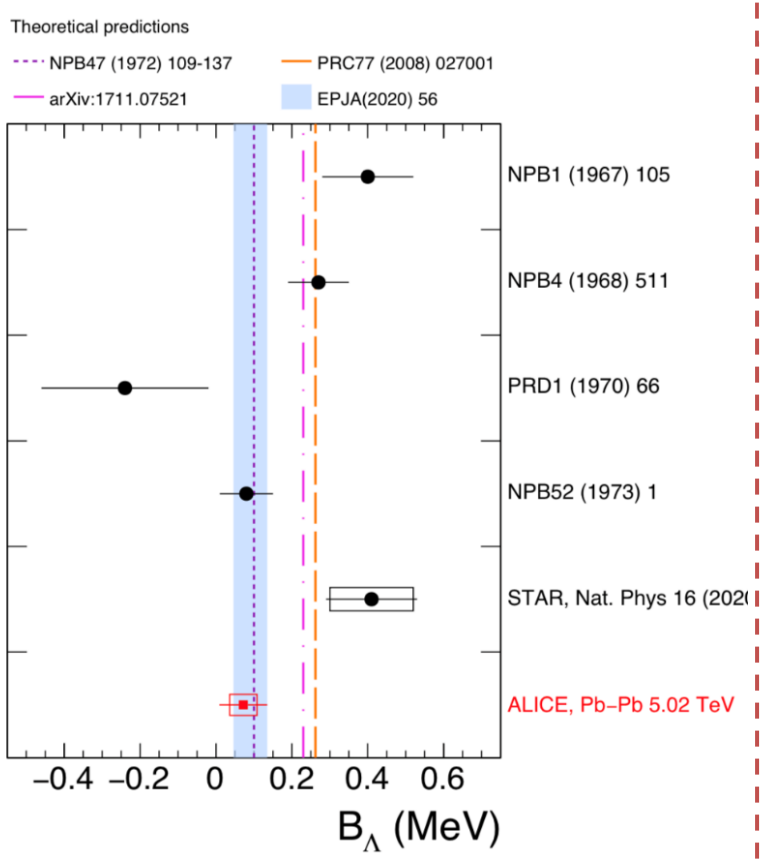
J. Chen et al., Phys. Rep. 760, 1 (2018);P. Braun-Munzinger and B. Donigus NPA987, 144 (2019)
D. N. Liu et al. Phys. Lett. B 855, 138855 (2024)

Lifetime, binding energy, and femtoscopy

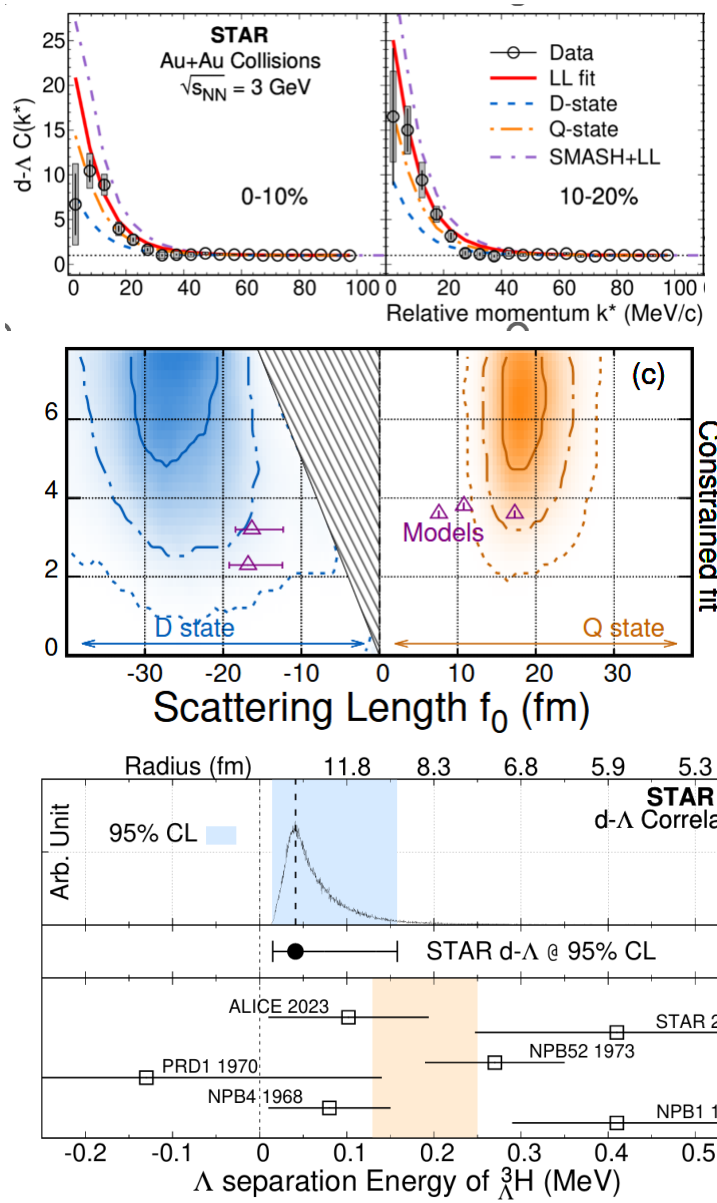
ALICE, PRL 131, 102302 (2023)

Y. G. Ma, Nucl. Sci. Tech. 3497 (2023)





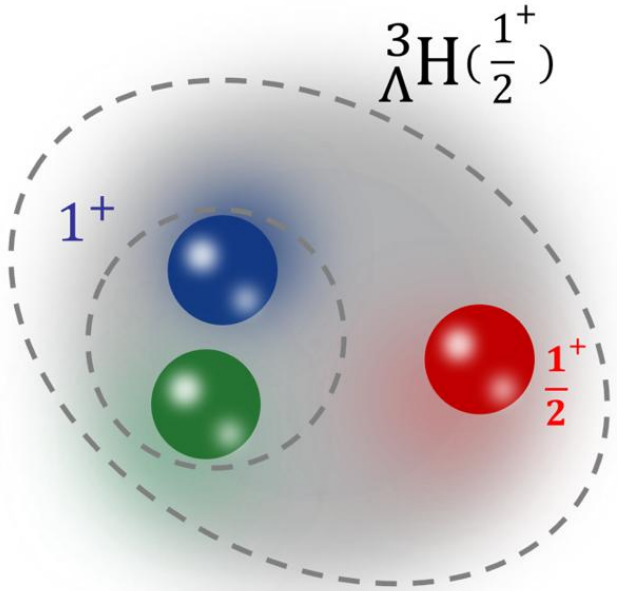
STAR, Phys. Rev. Lett. 136, 242303 (2026)



Spin of (anti-)hypertriton ?

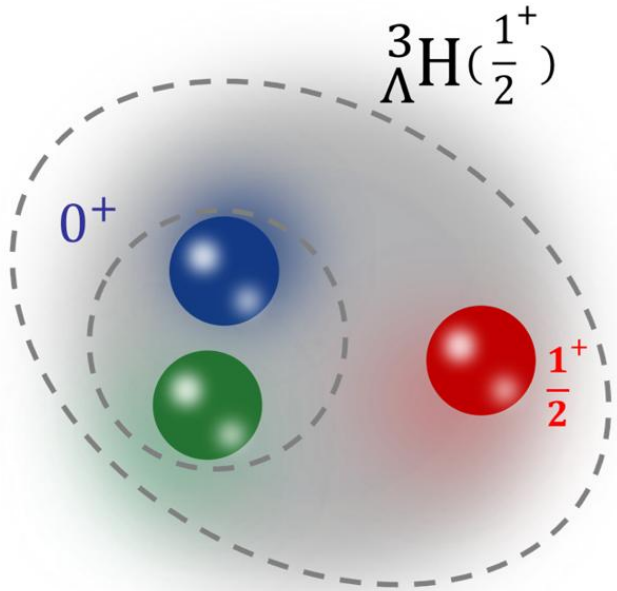
Nucleon pair: triplet

Total spin J = 1/2



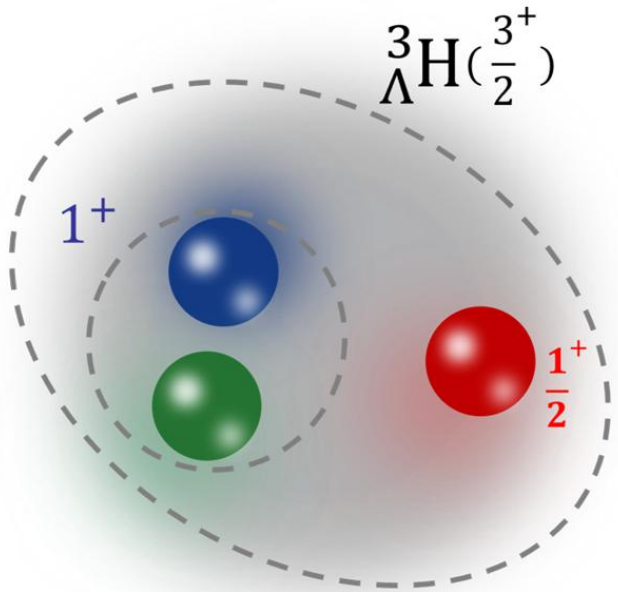
Nucleon pair: singlet

Total spin J = 1/2



Nucleon pair: triplet

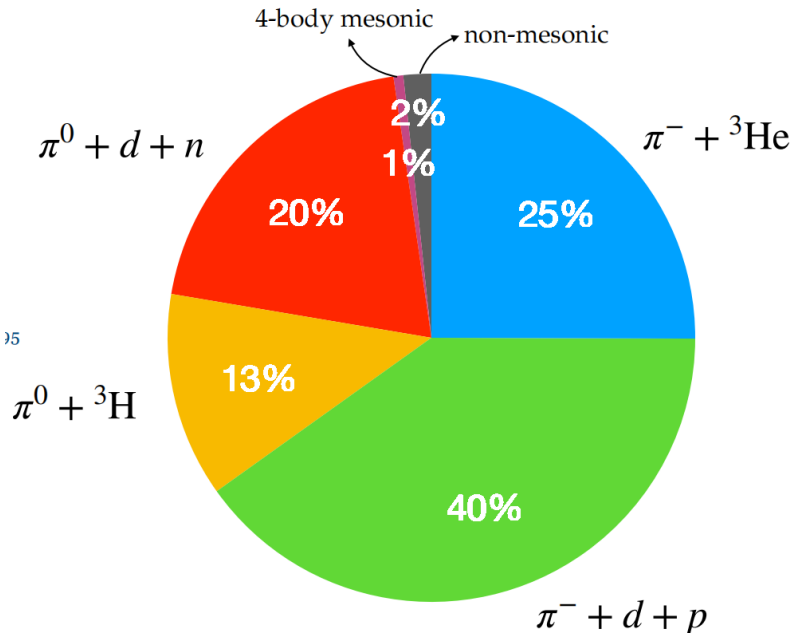
Total spin J = 3/2





Spin of (anti-)hypertriton ?

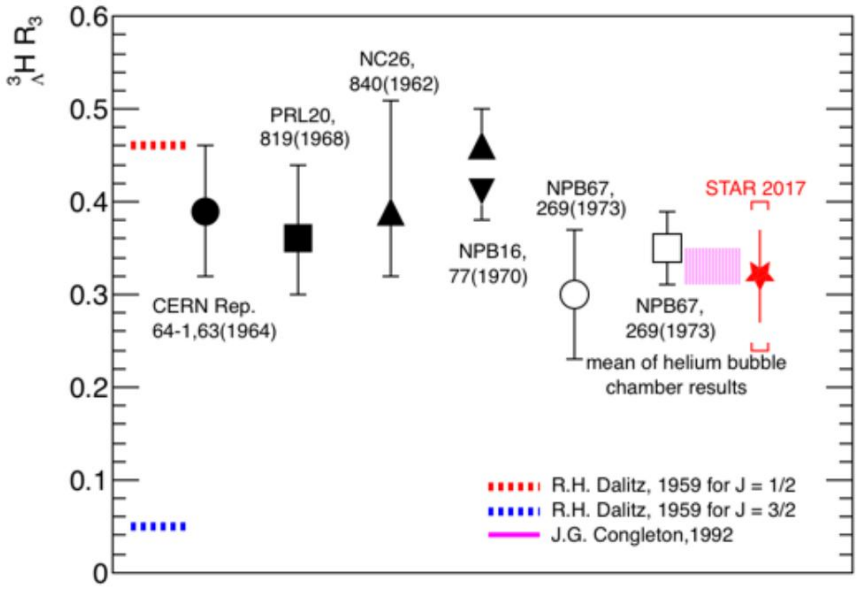
$$^3_\Lambda\mathrm{H} \mapsto \pi^- + {}^3\mathrm{He}, \qquad ^3_\Lambda\mathrm{H} \mapsto \pi^0 + {}^3\mathrm{H},$$
$$^3_\Lambda\mathrm{H} \mapsto \pi^- + d + p, \qquad ^3_\Lambda\mathrm{H} \mapsto \pi^0 + d + n,$$
$$^3_\Lambda\mathrm{H} \mapsto \pi^- + p + n + p, \qquad ^3_\Lambda\mathrm{H} \mapsto \pi^0 + p + n + n.$$



Relative branching ratio:

$$R_3 = \frac{\mathrm{B.R.}(^3_\Lambda\mathrm{H} \to {}^3\mathrm{He}\pi^-)}{\mathrm{B.R.}(^3_\Lambda\mathrm{H} \to {}^3\mathrm{He}\pi^-) + \mathrm{B.R.}(^3_\Lambda\mathrm{H} \to \mathrm{dp}\pi^-)}$$

STAR, PRC 97, 054909 (2018)



Favors spin 1/2

PHYSICAL REVIEW D **87,** 034506 (2013)

Light nuclei and hypernuclei from quantum chromodynamics in the limit of SU(3) flavor symmetry

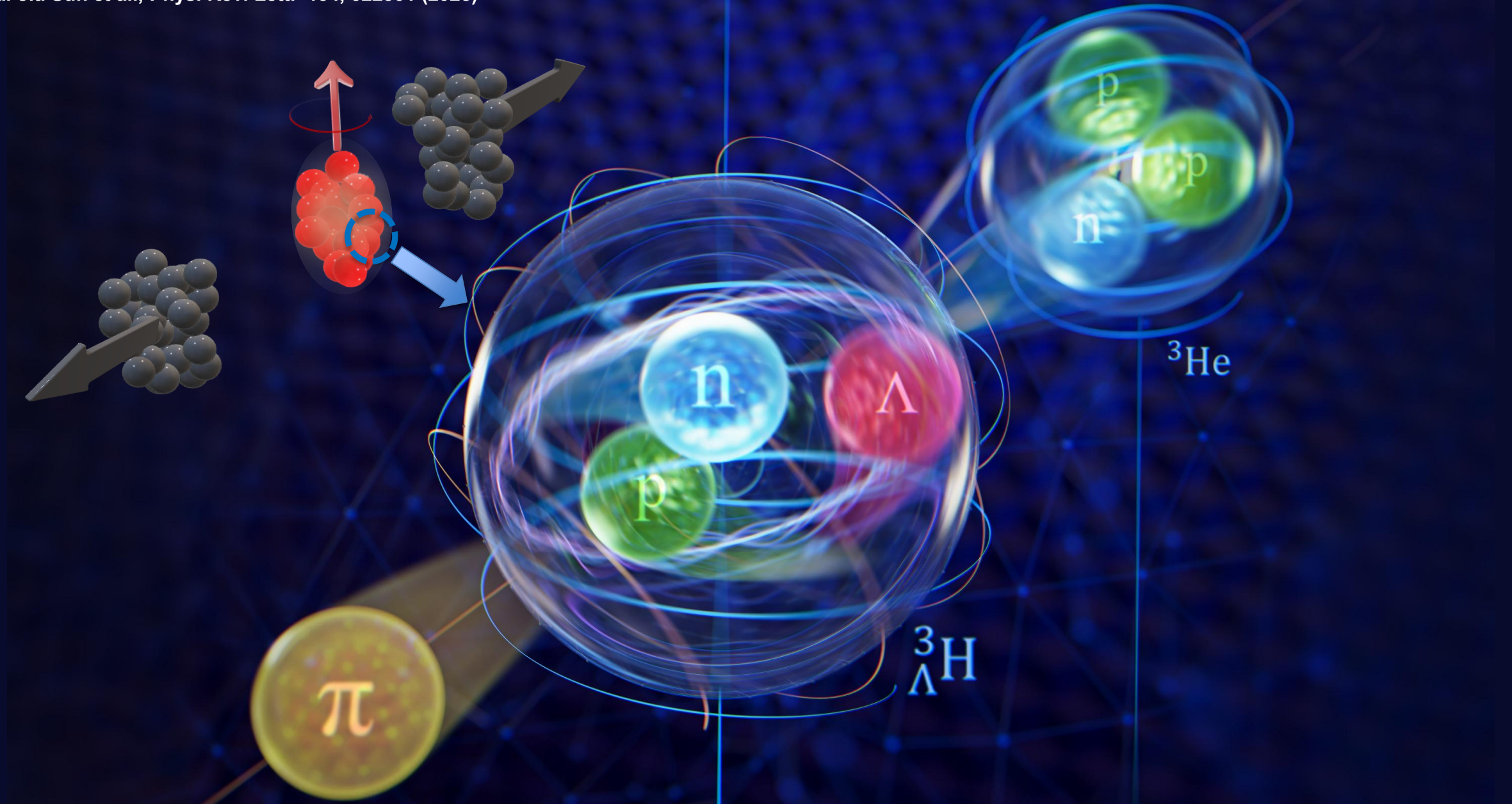
S. R. Beane,[1] E. Chang,[2] S. D. Cohen,[3] W. Detmold,[4,5] H. W. Lin,[3] T. C. Luu,[6] K. Orginos,[4,5] A. Parreño,[2] M. J. Savage,[3] and A. Walker-Loud[7,8]

Label	A	s	I	J^π	Local SU(3) irreps	This work
N	1	0	1/2	$1/2^+$	**8**	**8**
Λ	1	−1	0	$1/2^+$	**8**	**8**
Σ	1	−1	1	$1/2^+$	**8**	**8**
Ξ	1	−2	1/2	$1/2^+$	**8**	**8**
d	2	0	0	1^+	$\overline{\mathbf{10}}$	$\overline{\mathbf{10}}$
nn	2	0	1	0^+	**27**	**27**
$n\Lambda$	2	−1	1/2	0^+	**27**	**27**
$n\Lambda$	2	−1	1/2	1^+	$\mathbf{8}_A$, $\overline{\mathbf{10}}$	-
$n\Sigma$	2	−1	3/2	0^+	**27**	**27**
$n\Sigma$	2	−1	3/2	1^+	**10**	**10**
$n\Xi$	2	−2	0	1^+	$\mathbf{8}_A$	$\mathbf{8}_A$
$n\Xi$	2	−2	1	1^+	$\mathbf{8}_A$, **10**, $\overline{\mathbf{10}}$	-
H	2	−2	0	0^+	**1**, **27**	**1**, **27**
^{3}H, ^{3}H	3	0	1/2	$1/2^+$	$\overline{\mathbf{35}}$	$\overline{\mathbf{35}}$
$^3_\Lambda$H$(1/2^+)$	3	−1	0	$1/2^+$	$\overline{\mathbf{35}}$	-
$^3_\Lambda$H$(3/2^+)$	3	−1	0	$3/2^+$	$\overline{\mathbf{10}}$	$\overline{\mathbf{10}}$
$^3_\Lambda$He,$^3_\Lambda$H, $nn\Lambda$	3	−1	1	$1/2^+$	**27**, **35**	**27**, **35**
$^3_\Sigma$He	3	−1	1	$3/2^+$	**27**	**27**
^{4}He	4	0	0	0^+	$\overline{\mathbf{28}}$	$\overline{\mathbf{28}}$
$^4_\Lambda$He, $^4_\Lambda$H	4	−1	1/2	0^+	$\overline{\mathbf{28}}$	-
$^4_{\Lambda\Lambda}$He	4	−2	1	0^+	**27**, $\overline{\mathbf{28}}$	**27**, $\overline{\mathbf{28}}$
$\Lambda\Xi^0pnn$	5	−3	0	$3/2^+$	$\overline{\mathbf{10}} + \cdots$	$\overline{\mathbf{10}}$

Favors spin 3/2

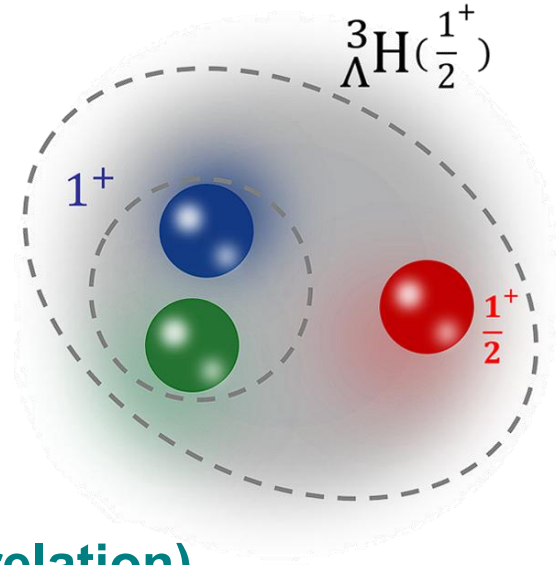
Deciphering the spin configuration of (anti-)hypertriton from its polarization

Kai-Jia Sun et al., Phys. Rev. Lett. 134, 022301 (2025)



Spin-dependent coalescence model

Kai-Jia Sun et al., Phys. Rev. Lett. 134, 022301 (2025)



➢ Spin wavefunction

$$
\begin{aligned}
|\tfrac{1}{2},\uparrow\rangle_{^3_\Lambda\mathrm{H}} &= \frac{\sqrt{6}}{3}|\tfrac{1}{2},\tfrac{1}{2}\rangle_n|\tfrac{1}{2},\tfrac{1}{2}\rangle_p|\tfrac{1}{2},-\tfrac{1}{2}\rangle_\Lambda \\
&- \frac{\sqrt{6}}{6}(|\tfrac{1}{2},\tfrac{1}{2}\rangle_n|\tfrac{1}{2},-\tfrac{1}{2}\rangle_p|\tfrac{1}{2},\tfrac{1}{2}\rangle_\Lambda \\
&+ |\tfrac{1}{2},-\tfrac{1}{2}\rangle_n|\tfrac{1}{2},\tfrac{1}{2}\rangle_p|\tfrac{1}{2},\tfrac{1}{2}\rangle_\Lambda),
\end{aligned}
\qquad
\begin{aligned}
|\tfrac{1}{2},\downarrow\rangle_{^3_\Lambda\mathrm{H}} &= -\frac{\sqrt{6}}{3}|\tfrac{1}{2},-\tfrac{1}{2}\rangle_n|\tfrac{1}{2},-\tfrac{1}{2}\rangle_p|\tfrac{1}{2},\tfrac{1}{2}\rangle_\Lambda \\
&+ \frac{\sqrt{6}}{6}(|\tfrac{1}{2},\tfrac{1}{2}\rangle_n|\tfrac{1}{2},-\tfrac{1}{2}\rangle_p|\tfrac{1}{2},-\tfrac{1}{2}\rangle_\Lambda \\
&+ |\tfrac{1}{2},-\tfrac{1}{2}\rangle_n|\tfrac{1}{2},\tfrac{1}{2}\rangle_p|\tfrac{1}{2},-\tfrac{1}{2}\rangle_\Lambda).
\end{aligned}
$$

➢ Coalescence model for hypertriton production (without baryon spin correlation)

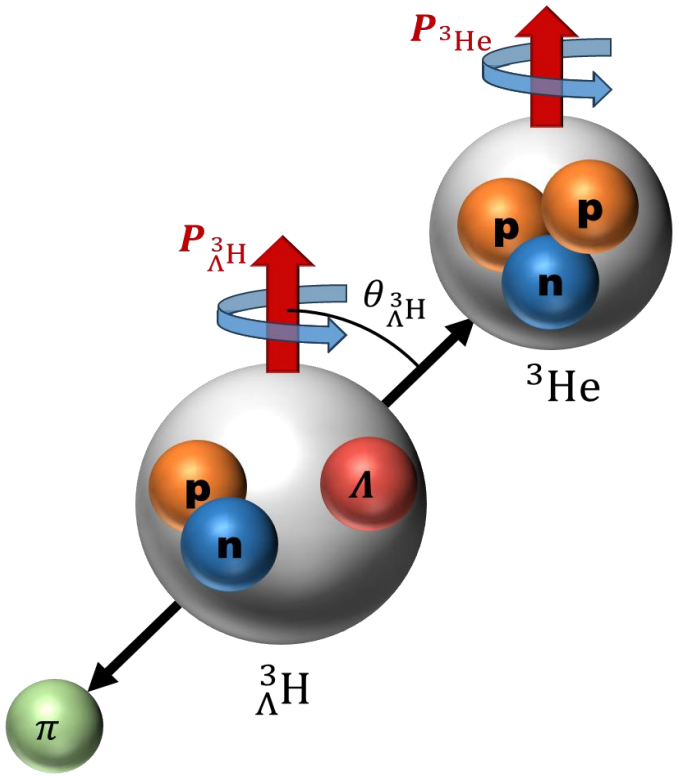
$$
\begin{aligned}
\hat{\rho}_{np\Lambda} &= \hat{\rho}_n \otimes \hat{\rho}_p \otimes \hat{\rho}_\Lambda \\
E\frac{\mathrm{d}^3N_{^3_\Lambda\mathrm{H},\pm\frac{1}{2}}}{\mathrm{d}\mathbf{P}^3} &= E\int \prod_{i=n,p,\Lambda} p_i^\mu \mathrm{d}^3\sigma_\mu \frac{\mathrm{d}^3p_i}{E_i} \bar{f}_i(\mathbf{x}_i,\mathbf{p}_i) \\
&\times \left(\frac{2}{3}w_{n,\pm\frac{1}{2}}w_{p,\pm\frac{1}{2}}w_{\Lambda,\mp\frac{1}{2}} + \frac{1}{6}w_{n,\pm\frac{1}{2}}w_{p,\mp\frac{1}{2}}w_{\Lambda,\pm\frac{1}{2}}\right. \\
&\left. + \frac{1}{6}w_{n,\mp\frac{1}{2}}w_{p,\pm\frac{1}{2}}w_{\Lambda,\pm\frac{1}{2}}\right) \\
&\times W_{^3_\Lambda\mathrm{H}}(\mathbf{x}_n,\mathbf{x}_p,\mathbf{x}_\Lambda;\mathbf{p}_n,\mathbf{p}_p,\mathbf{p}_\Lambda)\delta(\mathbf{P}-\sum_i \mathbf{p}_i)
\end{aligned}
$$

$$
\begin{aligned}
\mathcal{P}_{^3_\Lambda\mathrm{H}} &\approx \frac{\frac{2}{3}\mathcal{P}_n + \frac{2}{3}\mathcal{P}_p - \frac{1}{3}\mathcal{P}_\Lambda - \mathcal{P}_n\mathcal{P}_p\mathcal{P}_\Lambda}{1 - \frac{2}{3}(\mathcal{P}_n+\mathcal{P}_p)\mathcal{P}_\Lambda + \frac{1}{3}\mathcal{P}_n\mathcal{P}_p} \\
&\approx \frac{2}{3}\mathcal{P}_n + \frac{2}{3}\mathcal{P}_p - \frac{1}{3}\mathcal{P}_\Lambda \\
&\approx \mathcal{P}_\Lambda \qquad\qquad \mathcal{P}_p \approx \mathcal{P}_n \approx \mathcal{P}_\Lambda
\end{aligned}
$$

Assuming spin polarizations and correlations are small

(Anti-)hypertriton polarization and its spin structure

Hypertriton weak decay



Measured angular dependence

$$\frac{dN}{\mathrm{d}\ cos\theta^*} = \frac{1}{2}\left(1 + \alpha_{^3_\Lambda H}\mathcal{P}_{^3_\Lambda H} cos\theta^*\right)$$

$\mathcal{P}_{^3_\Lambda H}$: $^3_\Lambda H$ polarization

θ^* : Angle between ^3He momentum in $^3_\Lambda H$ rest frame

$\alpha_{^3_\Lambda H}$: $^3_\Lambda H$ decay parameter

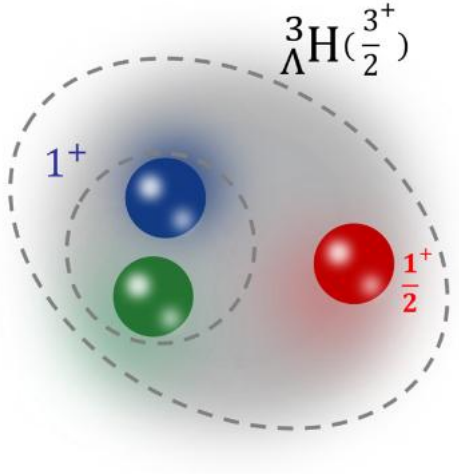
$$\alpha_{^3_\Lambda H} \approx -\frac{1}{3T_s^2 + \frac{1}{3}T_p^2}\alpha_\Lambda \approx -\frac{1}{2.58}\alpha_\Lambda$$

Sign flip !

For the J = 1/2, nucleon-triplet model shown, the analyzing coefficient changes sign relative to Lambda decay.

K.-J. Sun et al., Phys. Rev. Lett. 134, 022301 (2025); BESIII, Phys. Rev. Lett. 129, 131801 (2022).

(Anti-)hypertriton polarization and its spin structure

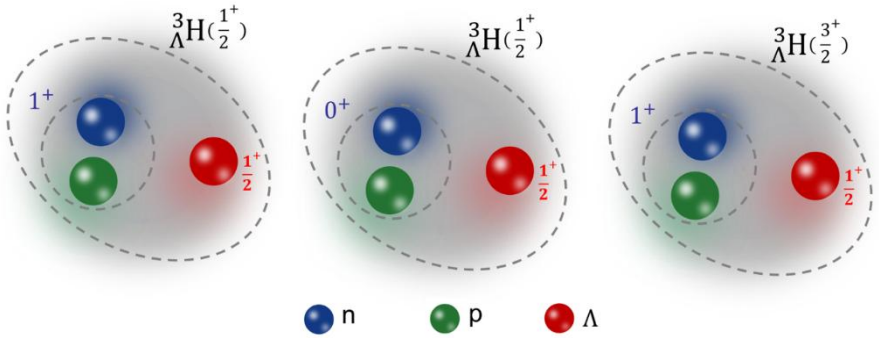


$$\hat{\rho}_{^3_\Lambda\mathrm{H}} \approx \mathrm{diag}\left[\frac{(1+\mathcal{P}_\Lambda)^3}{4(1+\mathcal{P}_\Lambda^2)}, \frac{(1-\mathcal{P}_\Lambda)(1+\mathcal{P}_\Lambda)^2}{4(1+\mathcal{P}_\Lambda^2)}, \frac{(1-\mathcal{P}_\Lambda)^2(1+\mathcal{P}_\Lambda)}{4(1+\mathcal{P}_\Lambda^2)}, \frac{(1-\mathcal{P}_\Lambda)^3}{4(1+\mathcal{P}_\Lambda^2)}\right]$$

$$T(^3_\Lambda\mathrm{H} \to \pi^- + {}^3\mathrm{He}) = \frac{FT_p}{\sqrt{6\pi}} \begin{pmatrix} e^{i\phi^*}\sin\theta^* & 0 \\ -\frac{2}{\sqrt{3}}\cos\theta^* & \frac{e^{i\phi^*}\sin\theta^*}{\sqrt{3}} \\ -\frac{e^{-i\phi^*}\sin\theta^*}{\sqrt{3}} & -\frac{2}{\sqrt{3}}\cos\theta^* \\ 0 & -e^{-i\phi^*}\sin\theta^* \end{pmatrix}$$

$$\frac{dN}{d\cos\theta^*} = \frac{1}{2}\left[1 + \left(\hat{\rho}_{\frac{1}{2},\frac{1}{2}} + \hat{\rho}_{-\frac{1}{2},-\frac{1}{2}} - \frac{1}{2}\right)(3\cos^2\theta^* - 1)\right]$$

$$\hat{\rho}_{\frac{1}{2},\frac{1}{2}} + \hat{\rho}_{-\frac{1}{2},-\frac{1}{2}} - \frac{1}{2} \approx -\frac{\mathcal{P}_\Lambda^2}{1+\mathcal{P}_\Lambda^2} \approx -\mathcal{P}_\Lambda^2$$

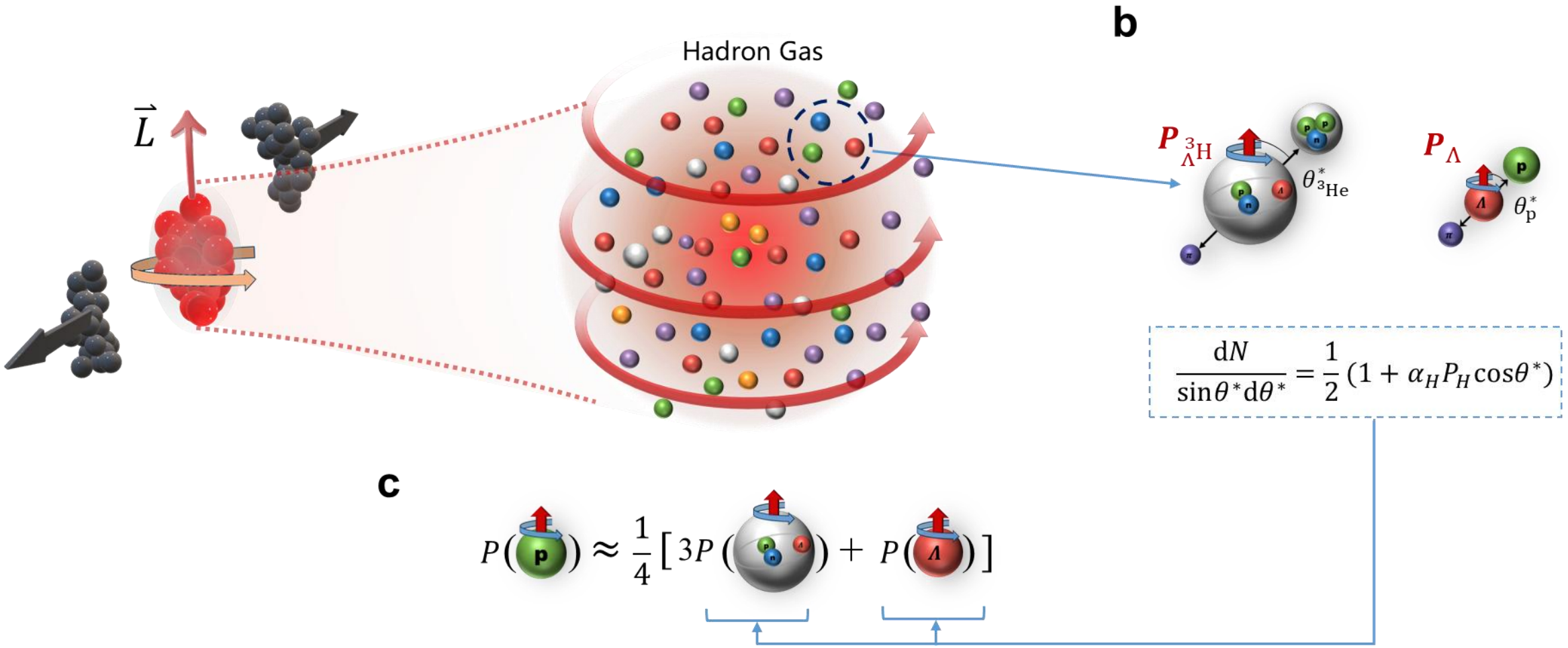


J^π	Structure	Decay mode	$dN/(\sin\theta^* d\theta^*)$
$\frac{1}{2}^+$	$\Lambda(\frac{1}{2}^+) - np(1^+)$	$^3_\Lambda\mathrm{H} \to \pi^- + {}^3\mathrm{He}$	$\frac{1}{2}[1 - (1/2.58)\alpha_\Lambda\mathcal{P}_\Lambda\cos\theta^*]$
$\frac{1}{2}^+$	$\Lambda(\frac{1}{2}^+) - np(0^+)$	$^3_\Lambda\mathrm{H} \to \pi^- + {}^3\mathrm{He}$	$\frac{1}{2}(1 + \alpha_\Lambda\mathcal{P}_\Lambda\cos\theta^*)$
$\frac{3}{2}^+$	$\Lambda(\frac{1}{2}^+) - np(1^+)$	$^3_\Lambda\mathrm{H} \to \pi^- + {}^3\mathrm{He}$	$\frac{1}{2}\left(1 - \mathcal{P}_\Lambda^2(3\cos^2\theta^* - 1)\right)$
$\frac{1}{2}^-$	$\bar{\Lambda}(\frac{1}{2}^-) - \overline{np}(1^+)$	$^3_{\bar{\Lambda}}\bar{\mathrm{H}} \to \pi^+ + {}^3\overline{\mathrm{He}}$	$\frac{1}{2}[1 - (1/2.58)\alpha_{\bar{\Lambda}}\mathcal{P}_{\bar{\Lambda}}\cos\theta^*]$
$\frac{1}{2}^-$	$\bar{\Lambda}(\frac{1}{2}^-) - \overline{np}(0^+)$	$^3_{\bar{\Lambda}}\bar{\mathrm{H}} \to \pi^+ + {}^3\overline{\mathrm{He}}$	$\frac{1}{2}(1 + \alpha_{\bar{\Lambda}}\mathcal{P}_{\bar{\Lambda}}\cos\theta^*)$
$\frac{3}{2}^-$	$\bar{\Lambda}(\frac{1}{2}^-) - \overline{np}(1^+)$	$^3_{\bar{\Lambda}}\bar{\mathrm{H}} \to \pi^+ + {}^3\overline{\mathrm{He}}$	$\frac{1}{2}\left(1 - \mathcal{P}_{\bar{\Lambda}}^2(3\cos^2\theta^* - 1)\right)$

Different polarization and decay patterns!

From measured weak decays to inferred proton polarization

D. N. Liu, Y. P. Zhen, W. H. Zhou, J. H. Chen, C. M. Ko, Y. G. Ma, and S. Zhang, Phys. Rev. Res. 8, 033057 (2026)



Energy dependence

Lambda

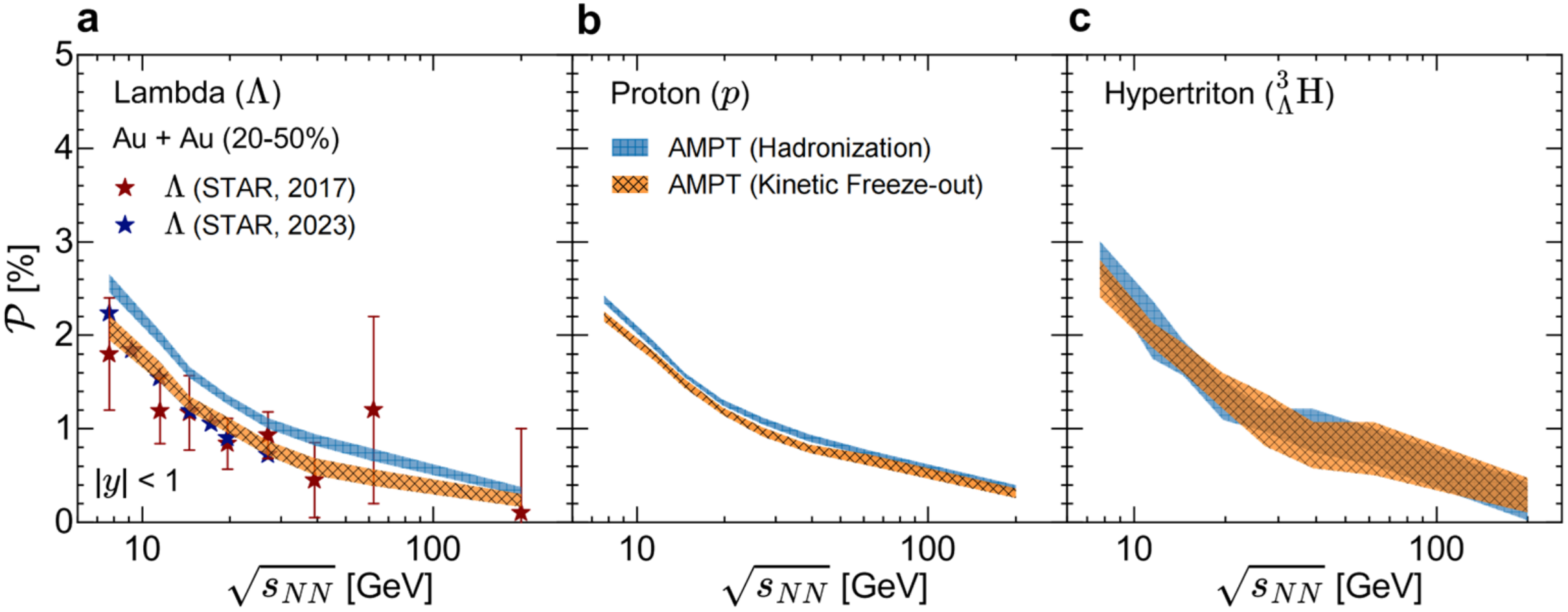
Data + transport calculation

Proton

Transport-model prediction

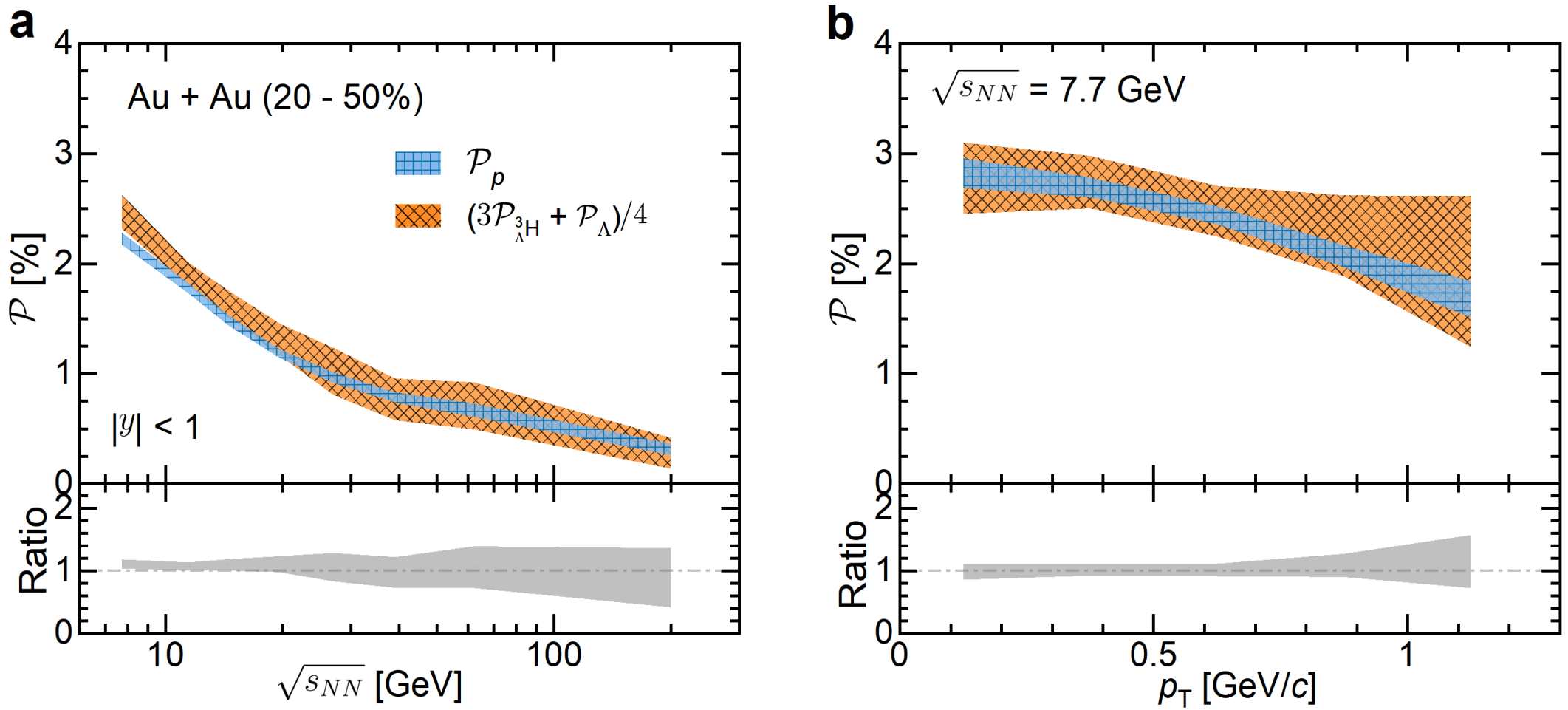
Hypertriton

Coalescence-model prediction



Dai-Neng Liu et al., Phys. Rev. Res. 8, 033057 (2026)

Decoding proton spin polarization



$$\mathcal{P}_p \approx \frac{1}{4}\left(3\mathcal{P}_{^3_\Lambda\mathrm{H}} + \mathcal{P}_\Lambda\right)$$

Proton spin polarization can be decoded from polarizations of hypertriton and Lambda hyperon

A direct observation of proton spin polarization requires a baryon polarimeter

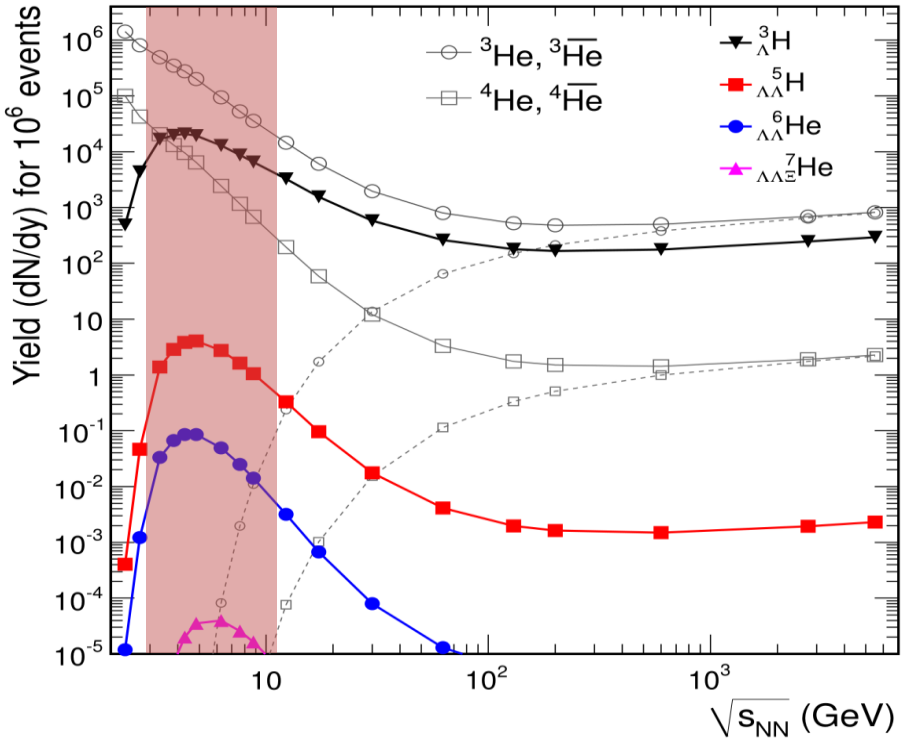
(see Y. T. Liang et al., Phys. Rev. D 112 (2025) 3, L031502)

Summary and outlook

01 **Geometry modulates spin polarization** — D. N. Liu et al., arXiv:2610.35310 (2026)

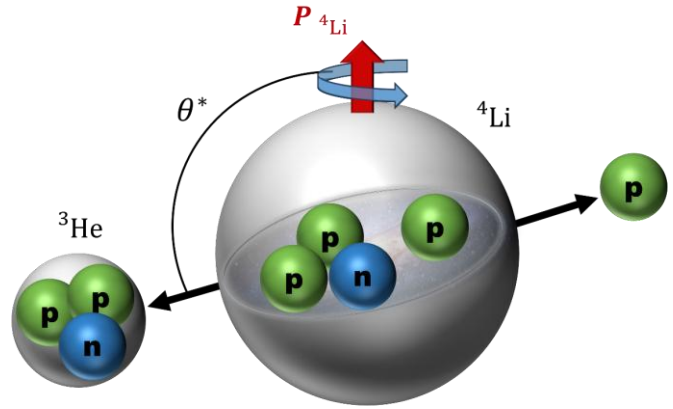
02 **Hypertriton polarization probes its spin structure** — K. J. Sun et al., Phys. Rev. Lett. 134, 022301 (2025)

03 **Joint measurements on Lambda and Hypertriton polarization can reveal how protons are polarized** — D. N. Liu et al., Phys. Rev. Res. 8, 033057 (2026)



A. Andronic et al., Phys. Lett. B 697, 203-207 (2011); **Y. P. Zheng et al., Phys. Rev. C 113, 054906 (2026)**

- FAIR/CBM (2.3-5.3 GeV)
- HIAF/CEE (2.1-4.5 GeV)
- NICA/MPD (4-11 GeV)
- J-PARC-HI (2-6.2 GeV)



Thank you for your attention.

Backup: Proton spin polarization

SU(6) quark coalescence model

Z. T. Liang and X. N. Wang PRL 94, 102301 (2005)

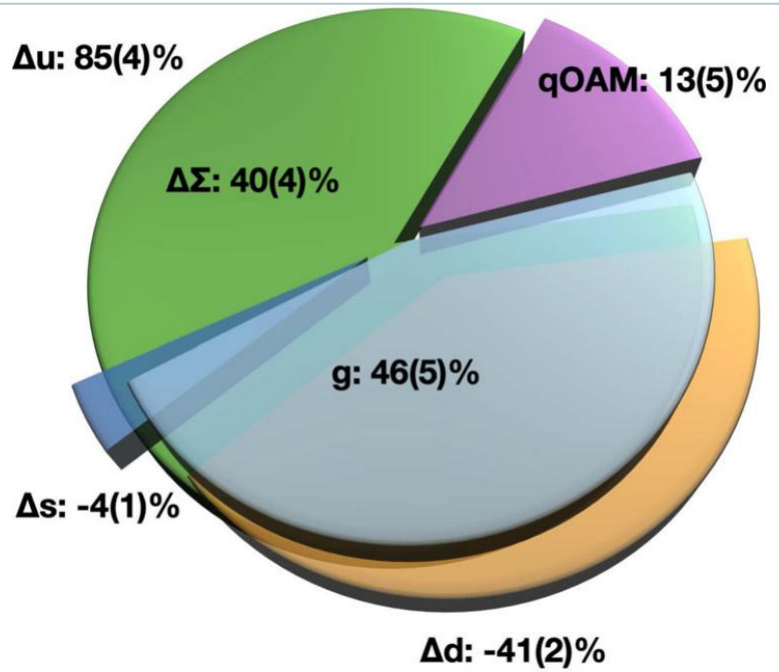
$$P_\Lambda = P_s$$

$$P_\Sigma = (4P_q - P_s - 3P_sP_q^2)/R_\Sigma, \quad R_\Sigma = 3 - 4P_qP_s + P_q^2;$$

$$P_\Xi = (4P_s - P_q - 3P_qP_s^2)/R_\Xi, \quad R_\Xi = 3 - 4P_qP_s + P_s^2;$$

$$P_\Omega = 2P_s(5 + P_s^2)/R_\Omega, \quad R_\Omega = 6(1 + P_s^2).$$

$$\mathcal{P}_p \approx (4\mathcal{P}_u - \mathcal{P}_d)/3$$



Frame-independent spin sum rule (Ji)

$$\frac{1}{2}\Delta\Sigma + L_q^z + J_g = \frac{\hbar}{2}$$

- $\Delta\Sigma/2$ and L_q^z (sum to J_q) are the quark helicity and OAM, respectively;
- Quark and gluon contributions J_q and J_g can be obtained from GPD moments;
- The sum rule also works for the transverse angular momentum in the IMF.

Infinite-momentum frame spin sum rule (Jaffe-Manohar)

$$\frac{1}{2}\Delta\Sigma + \Delta G + \ell_q + \ell_g = \frac{\hbar}{2}$$

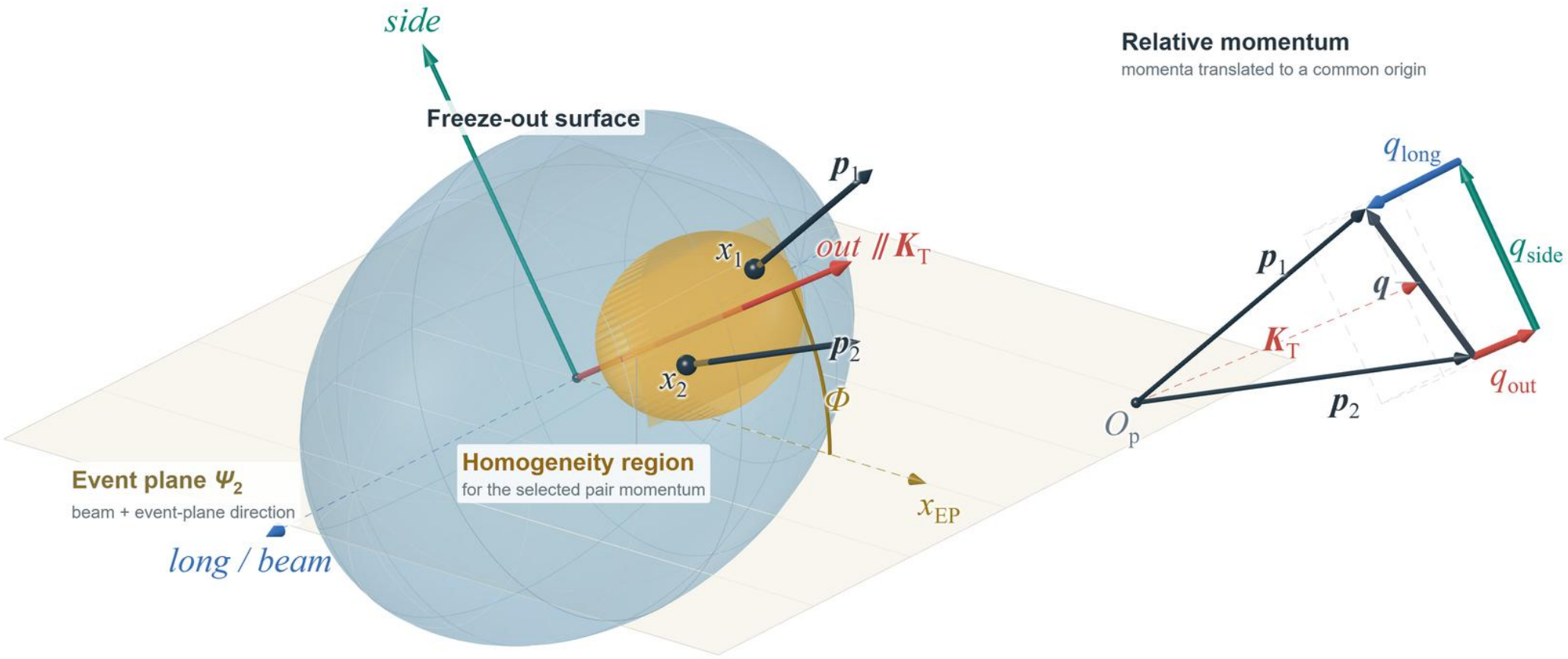
- ΔG is the gluon helicity, ℓ_q and ℓ_g are canonical OAM;
- All terms have partonic interpretations, ℓ_q and ℓ_g are twist-three quantities;
- ΔG is measurable from e.g. RHIC-spin and EIC; ℓ_q and ℓ_g can be extracted from GPDs.

X. D. Ji, F. Yuan, and Y. Zhao, Nature Rev. Phys. 3 (2021) 1, 27-38

Backup: out-side-long coordinates

Azimuthally sensitive HBT

Freeze-out geometry and relative momentum in the out-side-long frame



out ∥ K_T side = long × out long ∥ beam $\Phi = \varphi_{pair} - \Psi_2$ $q = p_1 - p_2$

LCMS. Spatial representation of freeze-out; schematic homogeneity region, not a measured source reconstruction.

Backup: Tilt angle and velocity profile in UrQMD

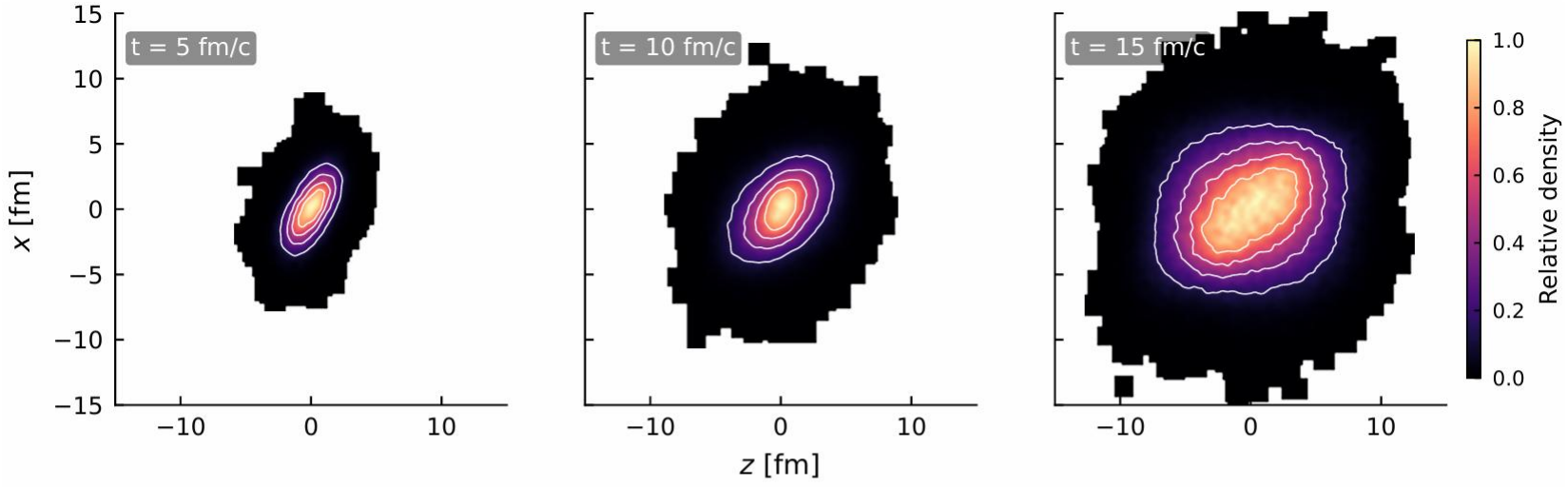


Fig. 5 The time evolution of pion shape.

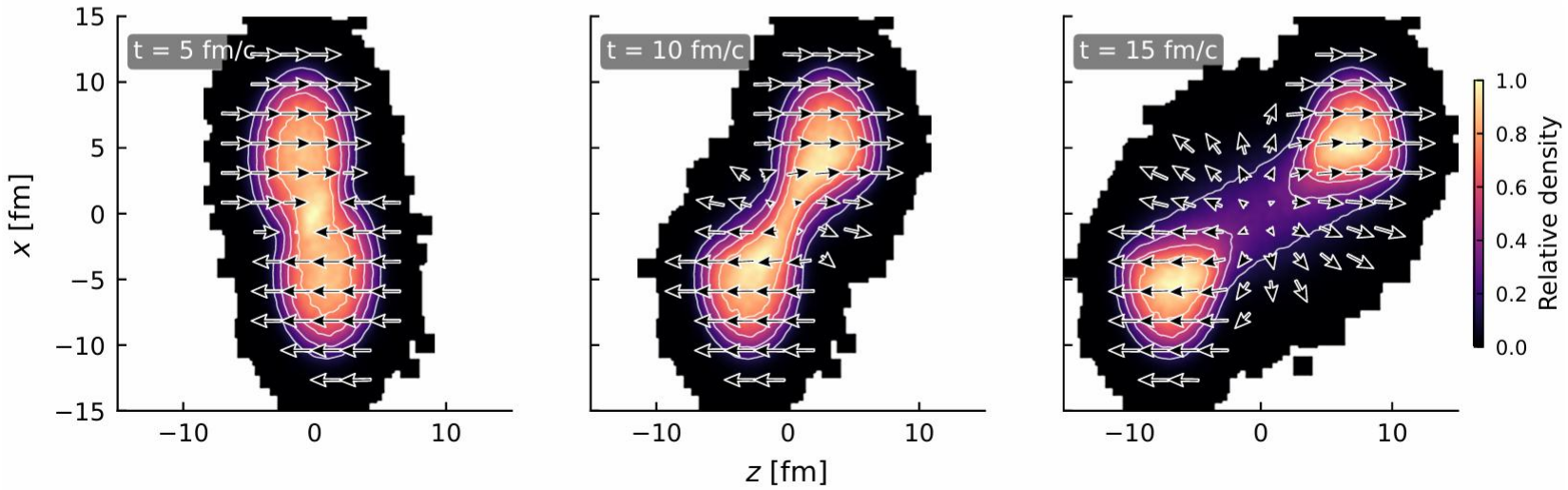


Fig. 6 The time evolution of proton shape and velocity profile. The longitudinal velocity v_z becomes larger along the x direction from center to out and it reaches the velocity of spectators.

Backup: tilt angle

PHYSICAL REVIEW C 111, 024902 (2025)

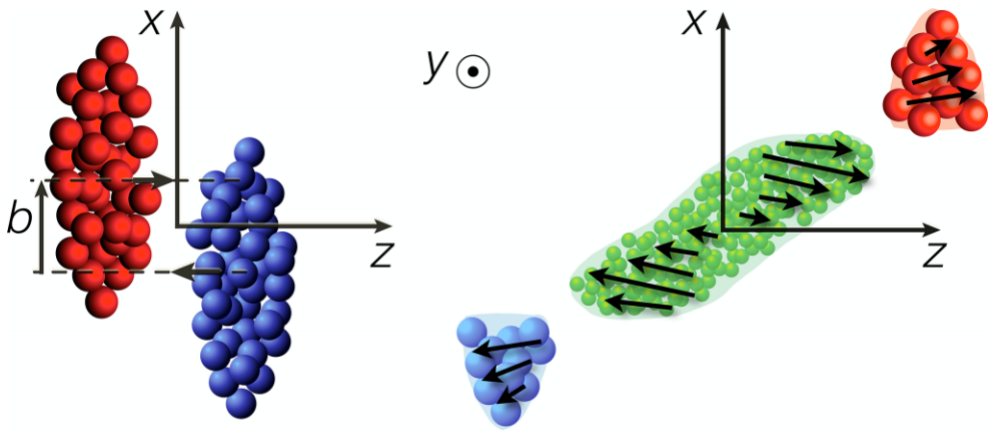
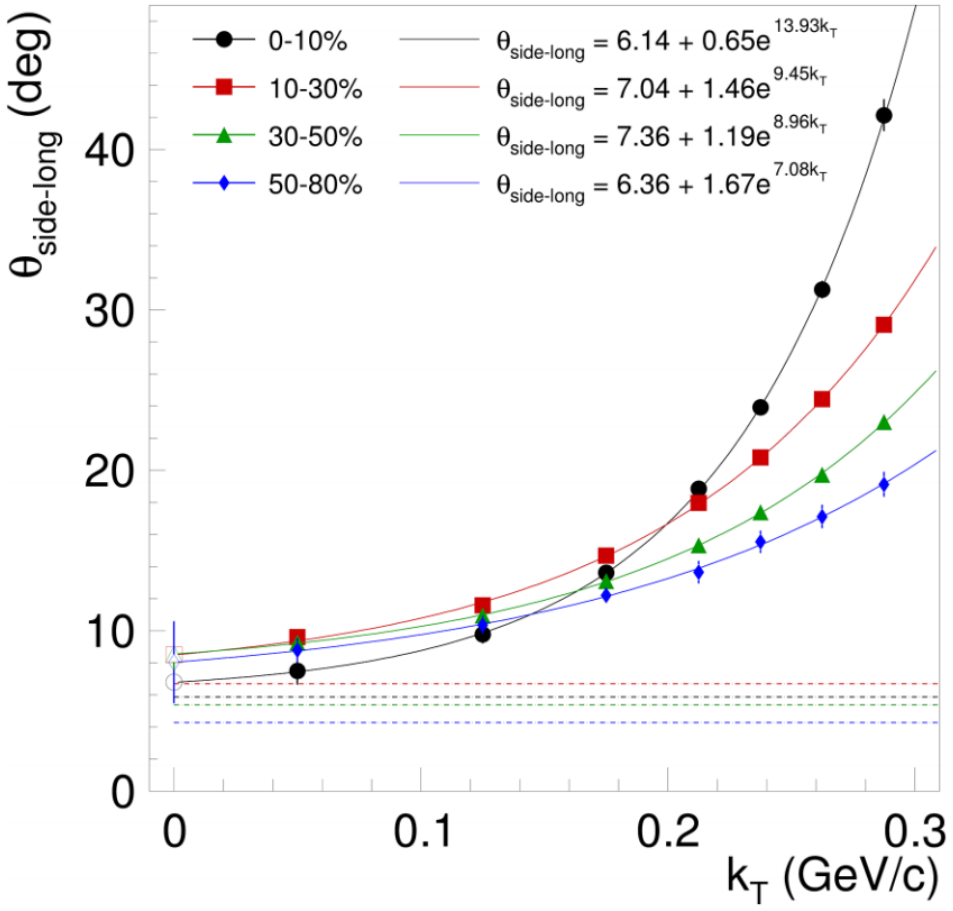
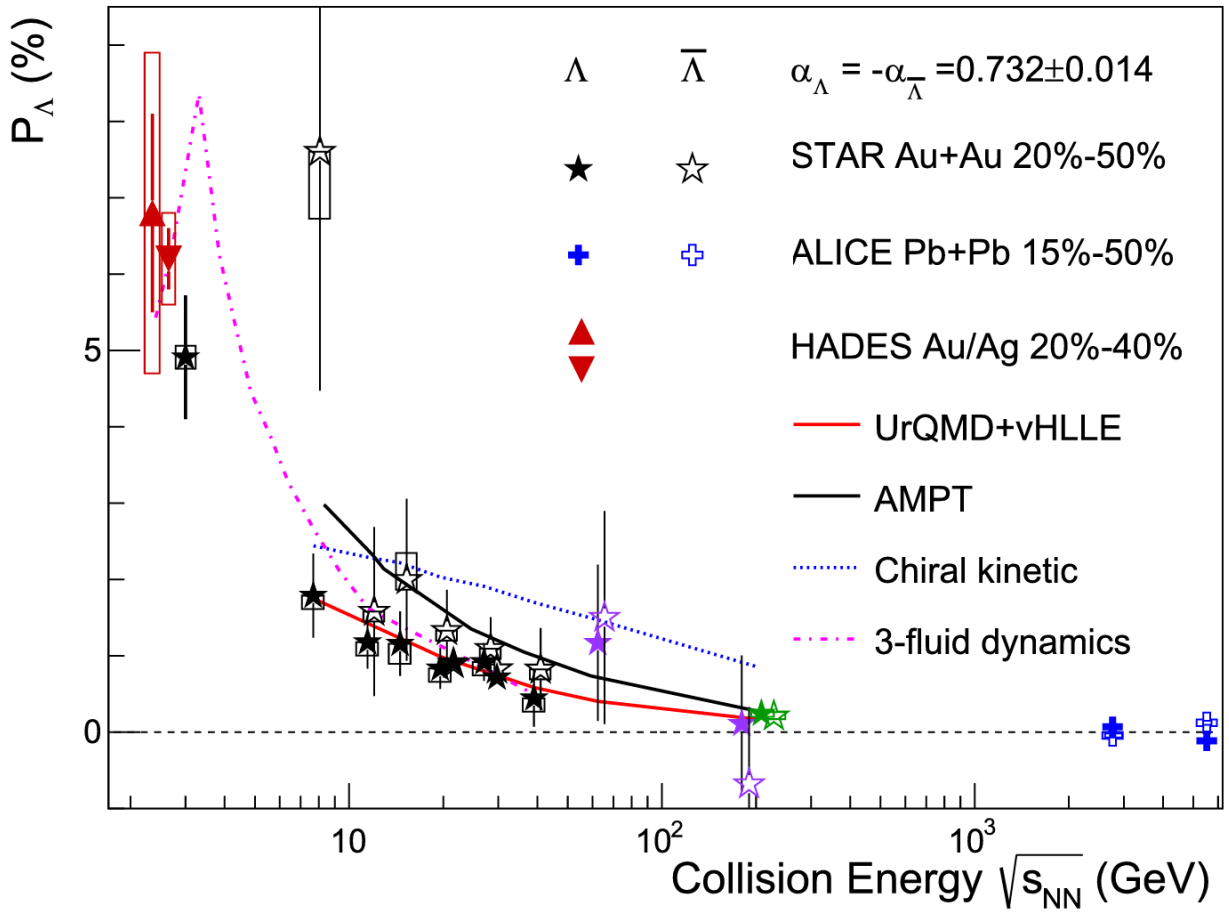


FIG. 1. Schematic view of the tilted emission source at the freeze-out time which appears in the noncentral collisions.



Backup: v1

J. Chen et al., Nucl. Sci. Tech. 35, 214 (2024)



STAR, Phys. Rev. Lett. 120, 062301 (2018)

